Science
AAAS

Supplementary Materials for

A COPII subunit acts with an autophagy receptor to target endoplasmic reticulum for degradation

Yixian Cui, Smriti Parashar, Muhammad Zahoor, Patrick G. Needham, Muriel Mari, Ming Zhu, Shuliang Chen, Hsuan-Chung Ho, Fulvio Reggiori, Hesso Farhan, Jeffrey L. Brodsky, and Susan Ferro-Novick*

Correspondence to: *sfnovick@ucsd.edu

This PDF file includes:

Materials and methods
Figures S1-S15
Tables S1-S2

Materials and methods

Strain construction and growth conditions.
The strains used in this study are listed in Supplementary Table S1. Yeast cells were cultured at 30˚C for all experiments. Genomic tags and disruptions were performed as described by Longtime et al. (*44*). The endogenous copies of Sec61, Rtn1, Per33, Atg40, Atg39, Sec23, Sec13, Lst1 and Sec24 were tagged at their C-terminus with either 1xGFP, 3xGFP or 2xmCherry as specified in each Figure and legend. Cells were grown overnight to early log phase in either SC (0.67% YNB, 2% glucose, amino acids as needed) or YPD (1% yeast extract, 2% peptone, 2% glucose) medium and autophagy was induced with either SD-N (0.67% YNB without amino acids or ammonium sulfate, 2% glucose); YPL (1% yeast extract, 2% peptone, 2% lactate); SGD (0.67% YNB without amino acids, 3% glycerol, 0.1% glucose), or YTO medium (0.67% YNB supplemented with amino acids, 0.1% Tween-40, 0.1% oleic acid).

ER-phagy assays
ER-phagy was monitored by fluorescence microscopy or with a gel assay. Fluorescence was used to measure the translocation of GFP fusion proteins into the vacuole, while western blot analysis quantitatively measured vacuolar cleavage of each fusion protein studied. To induce ER-phagy with rapamycin, strains expressing GFP fusion proteins were cultured in SC media to early-log phase (OD_{600}=0.2) before rapamycin (200 ng/ml) was added to induce ER-phagy. The times used for each experiment are indicated in the Figures and legends. To induce ER-phagy by high OD_{600}, cells were cultured in synthetic media with a starting OD_{600} of 0.001. Samples were collected after 18 h (OD_{600}=0.5) and 48 h (OD_{600}=8), then analyzed by fluorescence microscopy and western blot analysis.

For the fluorescence assays, cells were imaged as described below, and the percent of cells with GFP in the vacuole/total number of cells examined was calculated for each sample. For cleavage and degradation assays, cells (2.5 OD_{600} units) were pelleted, resuspended in 0.1 M NaOH, and incubated for 5 min at room temperature. The samples were then centrifuged and heated in sample buffer for 5 min at 95˚C before western blot analysis was performed with anti-GFP (1:1,000, Roche, #1181446001), Lst1, Sec24 (*45, 46*) and Adh1 antibodies (1:10,000, Rockland Immunochemicals Inc, #100-4143). A second precipitation method, using trichloroacetic acid (TCA), was also used to confirm the cleavage of Rtn1-GFP and Lst1-GFP (*11*).

Yeast Fluorescence Microscopy
Cells were imaged at room temperature with a Zeiss Axio Imager Z1 fluorescence microscope using a 100x1.3 NA oil-immersion objective, and images were taken with a Zeiss AxioCam MRm digital camera and evaluated using AxioVision software.

For the Atg40 colocalization studies, Lst1-3xGFP, Sec23-GFP, Sec13-GFP or Sec24-GFP puncta completely colocalizing with non-cortical (clearly interior to the cortex) Atg40-2xmCherry puncta were quantitated at 0, 3 and 6 h of rapamycin treatment. A total of 200-300 GFP puncta were quantitated for each time point/experiment. Volocity software (PerkinElmer Inc.) was also used to obtain a Pearson's coefficient of colocalization for each cell.

Bulk autophagy assays

To monitor the cleavage of GFP-Atg8 in the vacuole, cells were grown overnight to early log phase, and incubated with rapamycin for 24 h at 30˚C. Samples were then processed for western blot analysis as described above.

To assay alkaline phosphatase activity (Pho8Δ60), cells were grown overnight in SC medium to an OD_{600}=0.6-0.8, shifted into SD-N medium for 0 or 4 h, and then assayed as described before (*15*).

Mitophagy, Pexophagy and the Cvt pathway

To monitor mitophagy, a GFP fusion to the mitochondrial outer membrane protein, Om45-GFP, was used (*47*). Cells expressing Om45-GFP were cultured in YPL medium to mid-log phase (OD_{600}=0.5), and then shifted to YPL medium (OD_{600}=0.1). After 72 h, the samples were analyzed by fluorescence microscopy and western blot analysis as described above.

Pexophagy was measured using a GFP fusion protein to a component of the peroxisomal importomer complex, Pex14 (*48*). Briefly, mid-log phase cells grown in YPD were subcultured to SGD (OD_{600}=0.2) medium and incubated for 16 h. YP medium (25 ml) was then added to 100 ml of the culture grown in SGD. After 4 h, cells were harvested, washed in sterile water, and resuspended in YTO and incubated for 19 h. Subsequently, half of the cells were shifted to SD-N and cultured for 6 h, while the remaining half served as a control. The samples were then analyzed by fluorescence microscopy and western blot analysis as described above.

To monitor Ape1 processing via the Cvt pathway, cells were grown in nutrient rich media to early log phase and lysed as described above. Processing was monitored by western blot analysis.

In Vitro Binding Assays

Yeast cells were cultured overnight in SC medium to an OD_{600}= 0.5 and then treated with 400 ng/ml rapamycin for 3 h. Lysates were prepared by converting 1200 OD_{600} units of cells to spheroplasts as described before (*15*) and the spheroplasts were lysed in 6.4 ml of lysis buffer (25 mM HEPES pH 7.4, 150 mM NaCl, 2 mM EDTA, 1 mM DTT, and 5× protease inhibitor cocktail). Subsequently, Triton X-100 was added to a final concentration of 0.5%, and the lysate was centrifuged at 16,000 × g for 15 min. The supernatant (2 mg) was removed and incubated for 1.5 h at room temperature with equimolar amounts (0.1 μM) of purified GST, GST–Lst1, GST–Sec24, GST-Sec23, or GST-Sec13 immobilized on beads. Afterwards, the beads were washed and eluted in SDS/PAGE sample buffer. The eluate was then fractionated on a 12% SDS polyacrylamide gel and immunoblot analysis was performed using the ECL method. Anti-FLAG antibody was used at 1:3,000 dilution (Sigma Aldrich, F3165).

Electron Microscopy

Cells were grown overnight in SC medium before inducing ER-phagy with 200 ng/ml rapamycin for 12 h. At the end of the incubation, the cells were processed for electron microscopy as previously described (*49*). Briefly, cells were fixed in potassium permanganate and embedded in Spuur's resin. After polymerization, 55-60 nm thin sections were cut using an Ultracut ultramicrotome (Leica Microsystems) and transferred onto formvar carbon-coated copper grids and stained before viewing. Two grids, containing sections obtained from the same preparation, were statistically evaluated by counting 100 randomly selected cell profiles. The average number of autophagic bodies per cell section that contained at least one ER fragment (tubule or sheet)

was determined. In our EM preparations, the cortical ER appeared as well-defined electron dense (dark) tubules with a width of 3-5 nm. These tubules were distributed along the plasma membrane and were sometimes distinctively connected to the nuclear envelope. The ER fragments within autophagic bodies had a length of at least 25 nm and were identified based on this morphology.

ATZ or ATM induction

To induce the expression of ATZ or ATM, two different methods were used. Cells containing ATZ-pYES2, ATM- pYES2, or an empty vector were grown to log phase in SC–Ura medium with 2% glucose. Half of the culture was washed two times with sterile water, resuspended in SC–Ura medium with 2% galactose and incubated for 24 h at 30˚C with shaking to induce expression (method 1). Alternatively, an overnight culture was grown in 2% raffinose, and the next day the cells were washed in sterile water and resuspended in 2% galactose (OD_{600}˜0.02). After 30 h, the cells were harvested at an OD_{600}<1.0 (method 2). Both methods of induction yielded similar results.

Sucrose gradient analysis of ATZ and ATM

Two different methods, described above, were used to express either ATZ or ATM for sucrose gradient analysis. Similar results were obtained with both methods. For the data in Figs. 4D and S12C, cells were grown in 2% raffinose prior to the incubation with 2% galactose (method 2). Multiple transformants were analyzed for ATZ or ATM expression, and sucrose gradient analysis was performed as described before (*27*).

ATM and ATZ secretion assay protocol

Yeast cells transformed with either ATM-pYES2 or ATZ-pYES2 were grown overnight in selective medium with 4% raffinose, washed with sterile water, inoculated into 10 ml cultures of selective medium containing 2% galactose (initial OD_{600} of 0.1) and grown at 30˚C to an OD_{600} of 0.9-1.0 (~16 h). The secretion of ATM and ATZ was then assayed as previously described (*50*).

UPR assays

The UPR was measured using a plasmid (pRH1209) containing four tandem UPR response sequences fused to GFP (4xUPRE-GFP). pRH1209 was linearized with StuI and integrated into the *URA3* locus (*51*). To induce the UPR, cells containing the integrated plasmid were cultured in SC media to mid-log phase ($0D_{600}$=0.5) before 8 mM DTT was added. After 1 h, the relative intensity of the GFP *fluorescence* signal in cells was measured by *flow cytometry (BD, Accuri c6).*

qRT-PCR

To measure mRNA levels in yeast, cells were grown in SC media to mid-log phase. Total RNA was extracted using the RNeasy Mini kit (Qiagen, #74104), and reverse transcription was performed using the iScript™ Reverse Transcription Supermix (Bio-Rad, #1708840). Real-time PCR was performed using iTaq™ Universal SYBR Green Supermix (Bio-Rad, #172-5120).

For the mammalian cell experiments, U2OS cells were transfected with siRNAs and harvested after 72 h. RNA was extracted using GenElute™ Mammalian Total RNA Miniprep Kit (Sigma Aldrich, # RTN70), and reverse transcribed using High-Capacity cDNA Reverse

Transcription Kit (Thermo Fisher #4368814). Real-time PCR was performed with 9 ng of cDNA per reaction using Quantitect primers (Qiagen).

Mammalian ER-phagy assays

To construct 3xFLAG-FAM134B (pSFNB2285), human FAM134B (1.6 kb cDNA fragment) was amplified from pSFNB2275 (FAM134B (Clone ID: HsCD00334674), inserted into the EcoRI and XhoI restriction sites of pOTB7 and cloned into the unique EcoRI and KpnI restriction sites of p3xFLAG-CMV-7.1 (Sigma Aldrich, E7533).

For all assays, U2OS cells (ATCC, HTB-96) were seeded at a density of $2x10^5$ cells per well in a 6-well plate. All siRNAs used in this study are listed in Supplementary Table S2. Depletions were performed with siRNA from Dharmacon (Dharmacon siGenome-SMARTpool) and independently validated with siRNA from Qiagen (Qiagen Flexitube siRNA). The non-targeting siRNA from Dharmacon was used as the siRNA control. Briefly, 10 nM siRNAs were mixed with 6 µl of HiPerFect transfection reagent (Qiagen, #301707) in 100 µl of serum free DMEM and added to freshly plated cells. After 48 h, the cells were transfected with 0.7 µg of 3xFLAG-FAM134B using TransIT-LT1 (Mirus, MIR2306) according to the instructions of the manufacturer. The next day, (typically 66 h after transfection), cells were treated with 250 nM Torin2 (Sigma Aldrich, SML1224) for 6 h to induce ER-phagy. For immunofluorescence studies, cells were treated with 100 nM Bafilomycin A1 (Sigma Aldrich, B1793) during the last 90 min of the incubation. When autophagy was inhibited, the ULK1/2 inhibitor (2 µM), MRT68921 (Tocris, #5780), was added together with Torin2. After the incubation, cells were either lysed and processed for western blot analysis, or fixed and stained for immunofluorescence as described below. For immunoblotting, antibodies against FLAG (Cell Signaling, #147935, 1:1000 dilution), and β-Actin (Santa CruZ, SC-47778, 1:1000 dilution) were used.

To stain for FLAG-FAM134B and LAMP1, cells were fixed in 4% PFA for 6 min, washed with PBS, incubated in 50 mM NH_4Cl for 8 min at room temperature and then washed with PBS. Next, the cells were incubated in permeabilization buffer (0.05% saponin in PBS) for 10 min at room temperature, and then incubated in permeabilization buffer supplemented with 5% BSA for 1 h at room temperature to reduce non-specific binding. Subsequently, the cells were treated with mouse monoclonal anti-LAMP1 (Santa CruZ, SC-20011) and rabbit polyclonal anti-FLAG (Cell Signaling, #147935) antibodies for 1 h at room temperature. After this incubation, the cells were washed with permeabilization buffer and incubated for 1 h with Alexa 488 anti-rabbit (Life technology and Catalog # A11008.) and Alexa 568 anti-mouse (Life technology, catalog number A11004) antibodies. The coverslips were briefly rinsed with Milli-Q water and embedded in polyvinyl alcohol mounting medium (Sigma Aldrich, catalog # 10981). Fluorescence images were acquired on a LSM 700 confocal microscope using a Plan-Aphochromat 63x/1.40 Oil Ph3 M27 objective.

To stain for RTN3 and LAMP1, a similar protocol was applied as described above, except that cells were fixed in methanol (-20^0C) for 6 min. Mouse monoclonal antibody (Santa CruZ, SC-374599) was first used to label RTN3 and then two antibodies were directly applied, Alexa 488 anti-mouse antibody together with a rabbit anti-LAMP1 antibody coupled to Cy3 (Sigma Aldrich, L0419). All antibodies used in immunofluorescence staining were diluted 1:1000 with permeabilization buffer containing 1% BSA.

To calculate the pixel intensity of FAM134B inside LAMP1-labeled lysosomes, 3xFLAG-FAM134B expressing cells were quantified using CellProfiler 2.2.0. Briefly, the

intensity profiles of the images were re-scaled to the CellProfiler format, then the LAMP1 channel (red) was thresholded and segmented using the module “Identify Primary Objects” to generate a mask (TopHat) that was superimposed onto the FAM134B image (green channel), and the median intensity of the green channel was measured. By this method, all LAMP1 structures were scored, allowing us to generate a value for the pixel intensity of FAM134B (green channel) inside LAMP-labeled lysosomes (red channel). The value obtained for the DMSO control was set to 1. Image J was used to calculate the relative pixel intensity of RTN3 (green channel) inside LAMP1-labelled lysosomes (red channel) in a manner similar to what was done for FAM134B. In brief, a total of 20 lysosomes/cell, chosen in the red channel for each experiment, were quantified and the intensity of the RTN3 signal (green channel) inside the LAMP1-labelled lysosomes was analyzed. The value obtained for the DMSO control was set to 1.

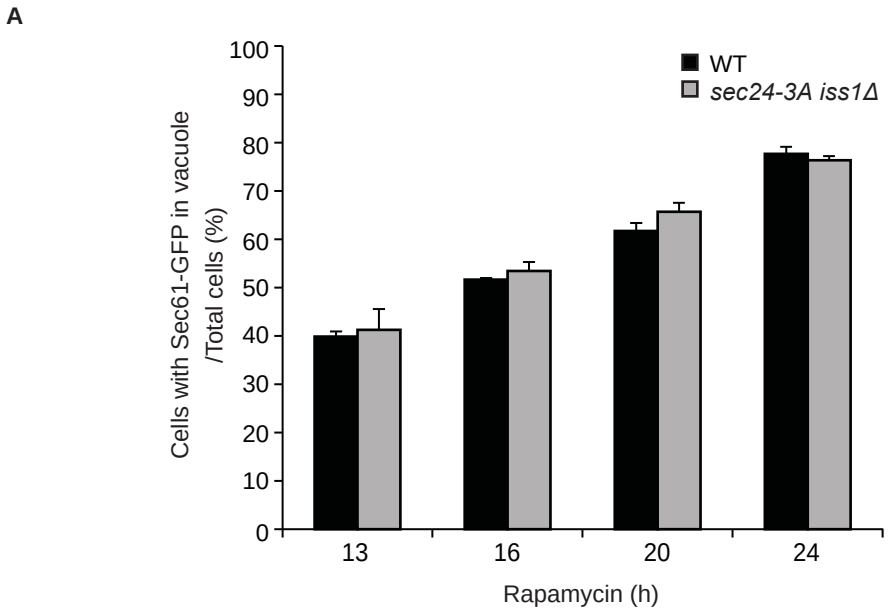
A
WT
sec24-3A iss1Δ
Cells with Sec61-GFP in vacuole /Total cells (%)
100
90
80
70
60
50
40
30
20
10
0
13
16
20
24
Rapamycin (h)

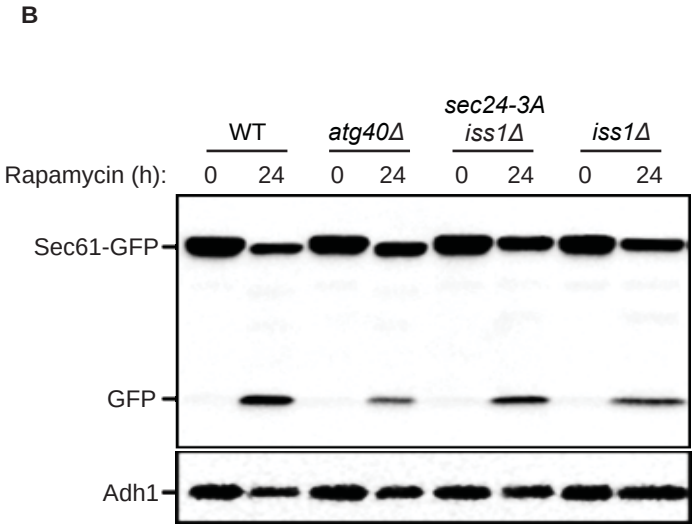
B
WT
atg40Δ
sec24-3A iss1Δ
iss1Δ
Rapamycin (h):
0
24
0
24
0
24
0
24
Sec61-GFP
GFP
Adh1

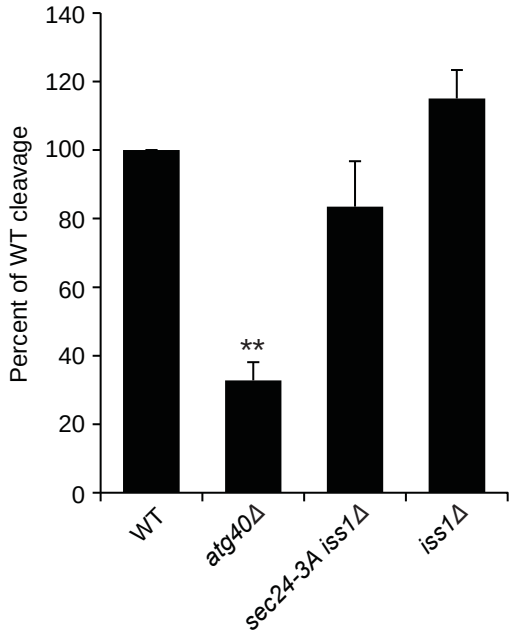
C
Percent of WT cleavage
140
120
100
80
60
40
20
0
**
WT
atg40Δ
sec24-3A iss1Δ
iss1Δ

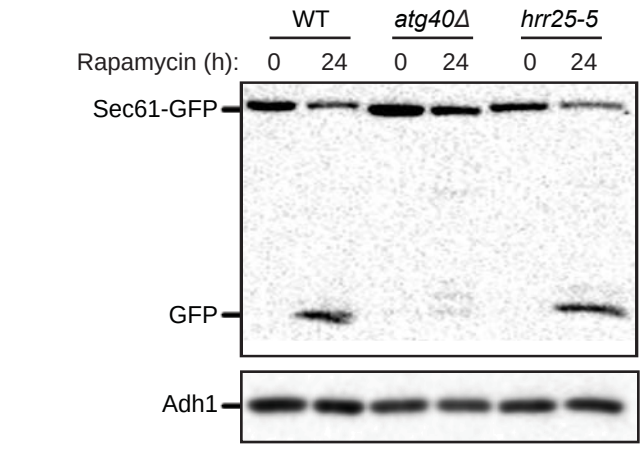
D
WT
atg40Δ
hrr25-5
Rapamycin (h):
0
24
0
24
0
24
Sec61-GFP
GFP
Adh1

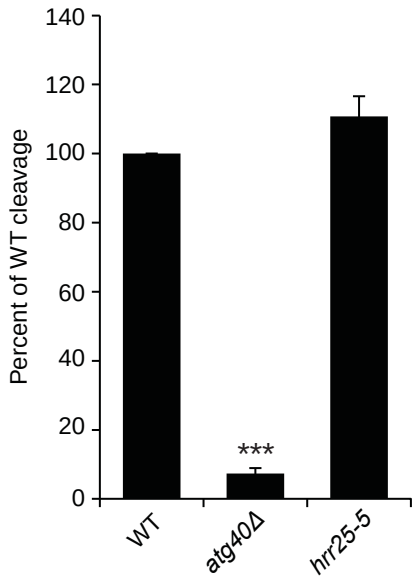
E
Percent of WT cleavage
140
120
100
80
60
40
20
0
***
WT
atg40Δ
hrr25-5

Figure S1. Sec24 phosphorylation by the CK1 kinase Hrr25 is dispensable for ER-phagy. (**A**) The percent of WT and *sec24-3A iss1Δ* cells with Sec61-GFP in the vacuole was quantitated by fluorescence at different time points after rapamycin treatment. (**B**) The cleavage of Sec61-GFP to GFP in WT, *atg40Δ*, *sec24-3A iss1Δ* and *iss1Δ* mutant strains was analyzed by immunoblotting using anti-GFP antibody. A representative blot from one of three experiments is shown. (**C**) Quantitation of the ratio of free GFP to Sec61-GFP for the data in (**B**). WT was set to 100%. (**D**) The cleavage of Sec61-GFP to GFP in WT, *atg40Δ* and the *hrr25-5* mutant was measured by immunoblotting using anti-GFP antibody. A representative blot from one of three experiments is shown. (**E**) Quantitation of the results in (**D**). Error bars in (**A**), (**C**) and (**E**) represent S.E.M., N=3; **P < 0.01, ***P < 0.001, Student's unpaired t-test.

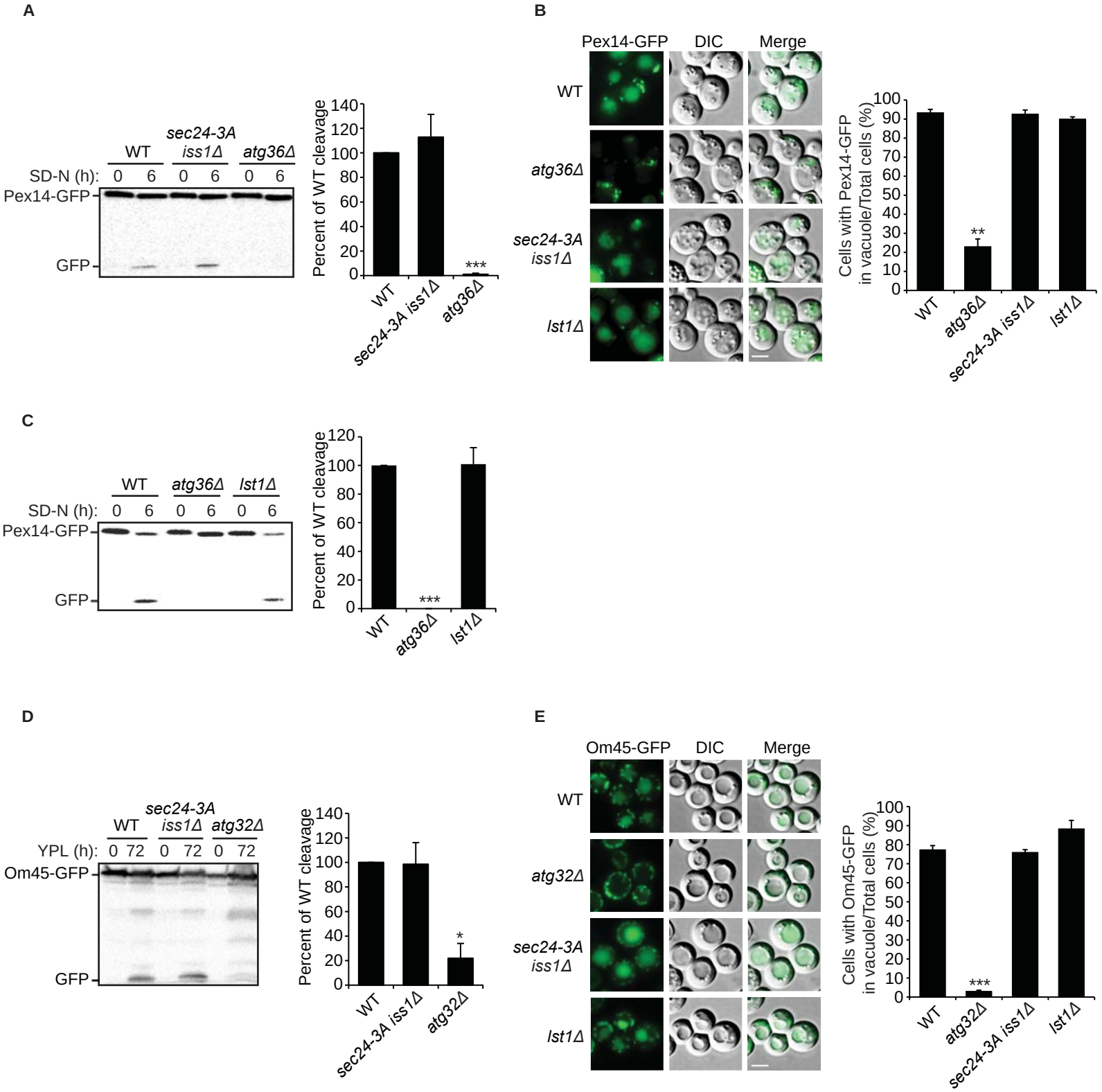
A
sec24-3A
WT
iss1Δ
atg36Δ
SD-N (h): 0 6 0 6 0 6
Pex14-GFP
GFP
Percent of WT cleavage
140
120
100
80
60
40
20
0
***
WT
sec24-3A iss1Δ
atg36Δ
B
Pex14-GFP
DIC
Merge
WT
atg36Δ
sec24-3A iss1Δ
lst1Δ
Cells with Pex14-GFP in vacuole/Total cells (%)
100
90
80
70
60
50
40
30
20
10
0
**
WT
atg36Δ
sec24-3A iss1Δ
lst1Δ
C
WT
atg36Δ
lst1Δ
SD-N (h): 0 6 0 6 0 6
Pex14-GFP
GFP
Percent of WT cleavage
120
100
80
60
40
20
0
***
WT
atg36Δ
lst1Δ
D
sec24-3A
WT
iss1Δ
atg32Δ
YPL (h): 0 72 0 72 0 72
Om45-GFP
GFP
Percent of WT cleavage
140
120
100
80
60
40
20
0
*
WT
sec24-3A iss1Δ
atg32Δ
E
Om45-GFP
DIC
Merge
WT
atg32Δ
sec24-3A iss1Δ
lst1Δ
Cells with Om45-GFP in vacuole/Total cells (%)
100
90
80
70
60
50
40
30
20
10
0
***
WT
atg32Δ
sec24-3A iss1Δ
lst1Δ
F
WT
atg32Δ
lst1Δ
YPL (h): 0 72 0 72 0 72
Om45-GFP
GFP
Percent of WT cleavage
200
180
160
140
120
100
80
60
40
20
0
***
WT
atg32Δ
lst1Δ
G
WT
atg1Δ
lst1Δ
prApe1
mApe1

Figure S2. Pexophagy, mitophagy and the Cvt pathway are Lst1-independent.
(**A-C**) Pexophagy was measured in WT, *sec24-3A iss1Δ, atg36Δ* and *lst1Δ* yeast by monitoring the cleavage of Pex14-GFP to GFP (**A** and **C**) and the translocation of Pex14-GFP to the vacuole by fluorescence (**B**). Western blot analysis was performed using anti-GFP antibody. A representative blot from one of three experiments is shown. In (**B**), the percent of cells with Pex14-GFP delivered to the vacuole was quantitated from 300 cells. (**D-F**) Mitophagy was assessed in WT, *sec24-3A iss1Δ*, *atg32Δ* and *lst1Δ* cells by measuring the cleavage of Om45-GFP to GFP by immunoblotting (**D** and **F**). A representative blot from one of three experiments is shown. (**E**) The translocation of Om45-GFP to the vacuole was detected by fluorescence microscopy, and the percent of cells with Om45-GFP delivered to the vacuole was quantitated from 300 cells. (**G**) The processing of precursor Ape1 (prApe1) to mature Ape1 (mApe1) via the Cvt pathway was assayed in WT, *atg1Δ* and *lst1Δ* cells by immunoblotting with anti-Ape1 antibody. Scale bars in (**B**) and (**E**), 5 μm. Error bars in (**A-F**) represent S.E.M., N=3; *P < 0.05, ** P < 0.01, *** P < 0.001, Student's unpaired t-test.

A

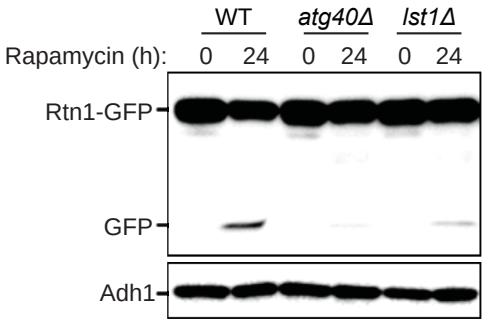
WT
atg40Δ
lst1Δ
Rapamycin (h):
0 24 0 24 0 24
Rtn1-GFP
GFP
Adh1

B

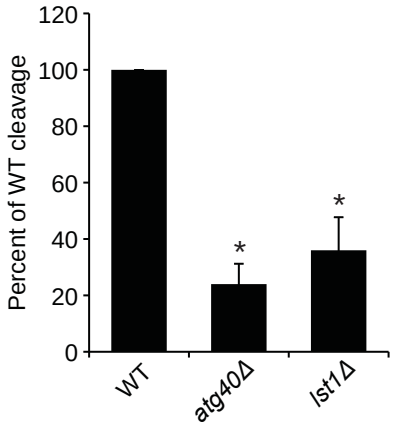
Percent of WT cleavage
120
100
80
60
40
20
0
*
*
WT
atg40Δ
lst1Δ

C

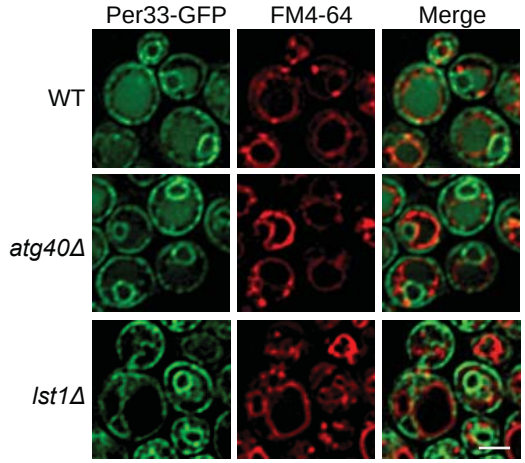
Per33-GFP
FM4-64
Merge
WT
atg40Δ
lst1Δ

D

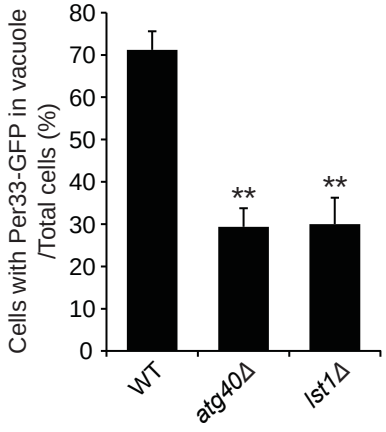
Cells with Per33-GFP in vacuole
/Total cells (%)
80
70
60
50
40
30
20
10
0
**
**
WT
atg40Δ
lst1Δ

E

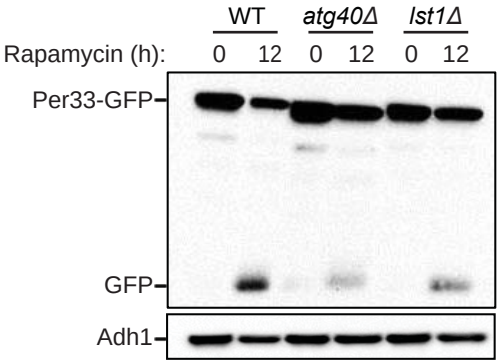
WT
atg40Δ
lst1Δ
Rapamycin (h):
0 12 0 12 0 12
Per33-GFP
GFP
Adh1

F

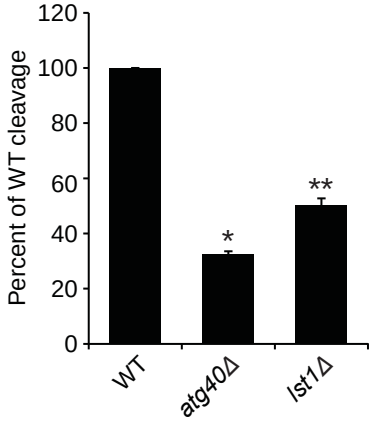
Percent of WT cleavage
120
100
80
60
40
20
0
*
**
WT
atg40Δ
lst1Δ

Figure S3. The degradation of Rtn1-GFP and Per33-GFP requires Lst1 in rapamycin-treated cells.

(**A**) The cleavage of Rtn1-GFP to GFP was analyzed in WT and mutant strains by immunoblotting with anti-GFP antibody. (**B**) Quantitation from three separate experiments of the ratio of free GFP to Rtn1-GFP from the data in **(A)**. (**C**) The translocation of Per33-GFP to the vacuole in WT, *atg40Δ* and *lst1Δ* cells was detected by fluorescence microscopy 24 h after rapamycin treatment. Scale bar, 5 μm. (**D**) The percent of cells with Per33-GFP delivered to the vacuole was quantitated by fluorescence from 300 cells. (**E**) The cleavage of Per33-GFP to GFP was analyzed in WT, *atg40Δ* and *lst1Δ* mutant strains by immunoblotting using anti-GFP antibody. A representative blot from three separate experiments is shown. (**F**) Quantitation of the ratio of free GFP to Per33-GFP for the data in (**E**). WT was set to 100%. Error bars in (**B**), (**D**) and (**F**) represent S.E.M., N=3; *P < 0.05, **P < 0.01, Student's unpaired t-test.

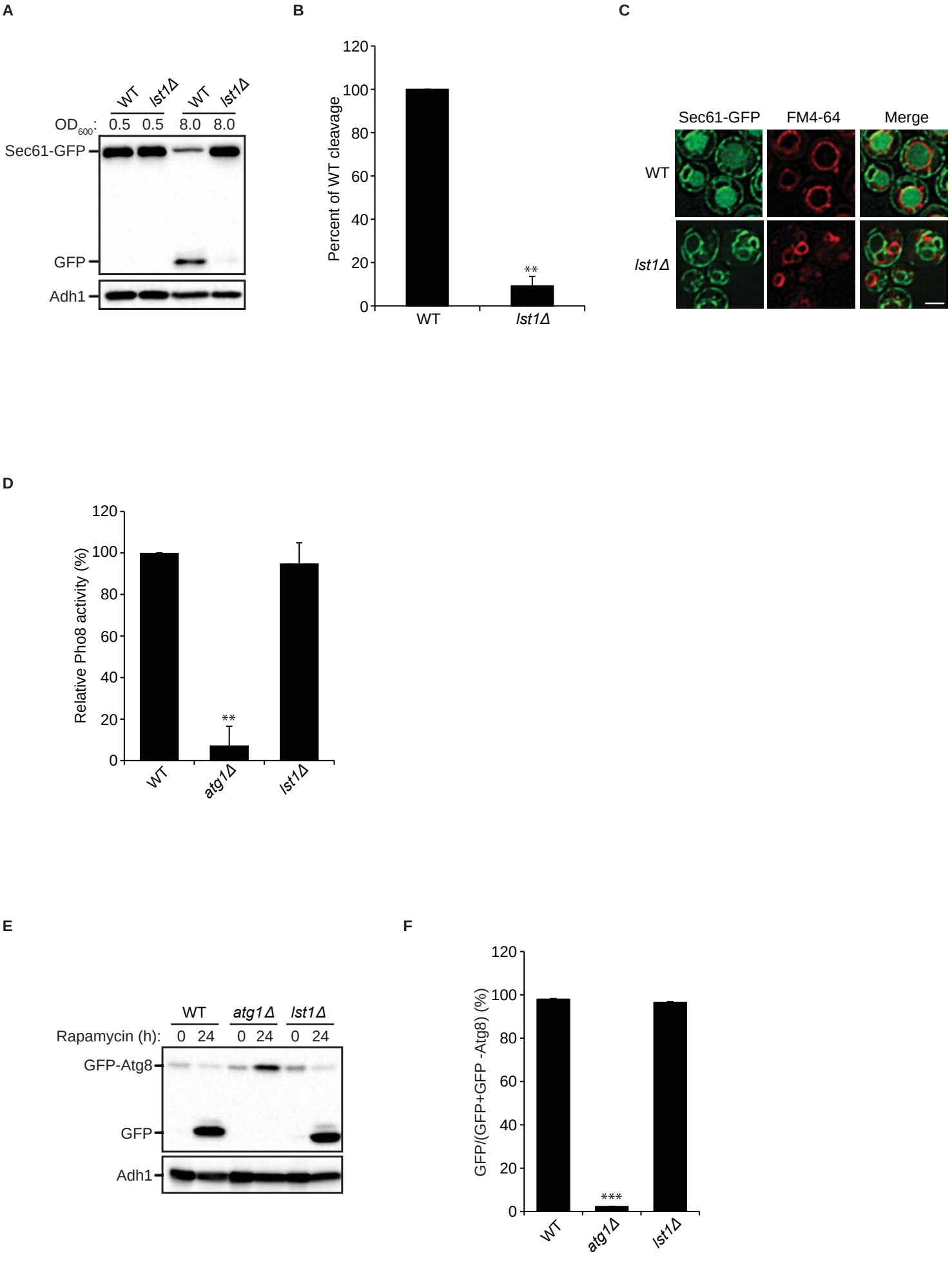
A
WT
lst1Δ
WT
lst1Δ
OD600: 0.5 0.5 8.0 8.0
Sec61-GFP
GFP
Adh1
B
Percent of WT cleavage
120
100
80
60
40
20
0
**
WT
lst1Δ
C
Sec61-GFP
FM4-64
Merge
WT
lst1Δ
D
Relative Pho8 activity (%)
120
100
80
60
40
20
0
**
WT
atg1Δ
lst1Δ
E
WT
atg1Δ
lst1Δ
Rapamycin (h): 0 24 0 24 0 24
GFP-Atg8
GFP
Adh1
F
GFP/(GFP+GFP -Atg8) (%)
120
100
80
60
40
20
0
***
WT
atg1Δ
lst1Δ

Figure S4. Lst1 is essential for ER-phagy, but not bulk autophagy.
(**A**) Lst1-mediated ER degradation was induced by high OD. The cleavage of Sec61-GFP to GFP was analyzed in WT and *lst1Δ* mutant strains by immunoblotting using anti-GFP antibody at 18 h (OD_{600}=0.5) and 48 h (OD_{600}=8) of growth in SC media. A representative blot from three experiments is shown. Adh1 was used as a loading control. (**B**) Quantitation of the ratio of free GFP to Sec61-GFP for the data in (**A**). WT was set to 100%. (**C**) Fluorescence microscopy 48 h after growth in SC media showing that Sec61-GFP is delivered to the vacuole for degradation at high OD. Scale bar in (**C**), 5 μm. (**D**) Lst1 is not required for bulk autophagy. To quantitatively assess bulk autophagy, vacuolar alkaline phosphatase activity (Pho8Δ60) was assayed in WT, *atg1Δ* and *lst1Δ* cells after nitrogen starvation. The data were normalized to WT. (**E-F**) Bulk autophagy was also assessed in WT, *atg1Δ* and *lst1Δ* strains at 0 and 24 h after rapamycin treatment by measuring the cleavage of GFP-Atg8 to GFP by western blot analysis. A representative blot **(E)** from one of three separate experiments is shown with Adh1 as a loading control. Extensive degradation of GFP-Atg8 to GFP was observed because of the long incubation time with rapamycin. Quantitation **(F)** of the ratio of free GFP to total GFP (GFP+GFP-Atg8) in **(E)**. Error bars in (**B**), (**D**) and (**F**) represent S.E.M., N=3; **P < 0.01, *** P < 0.001, Student's unpaired t-test.

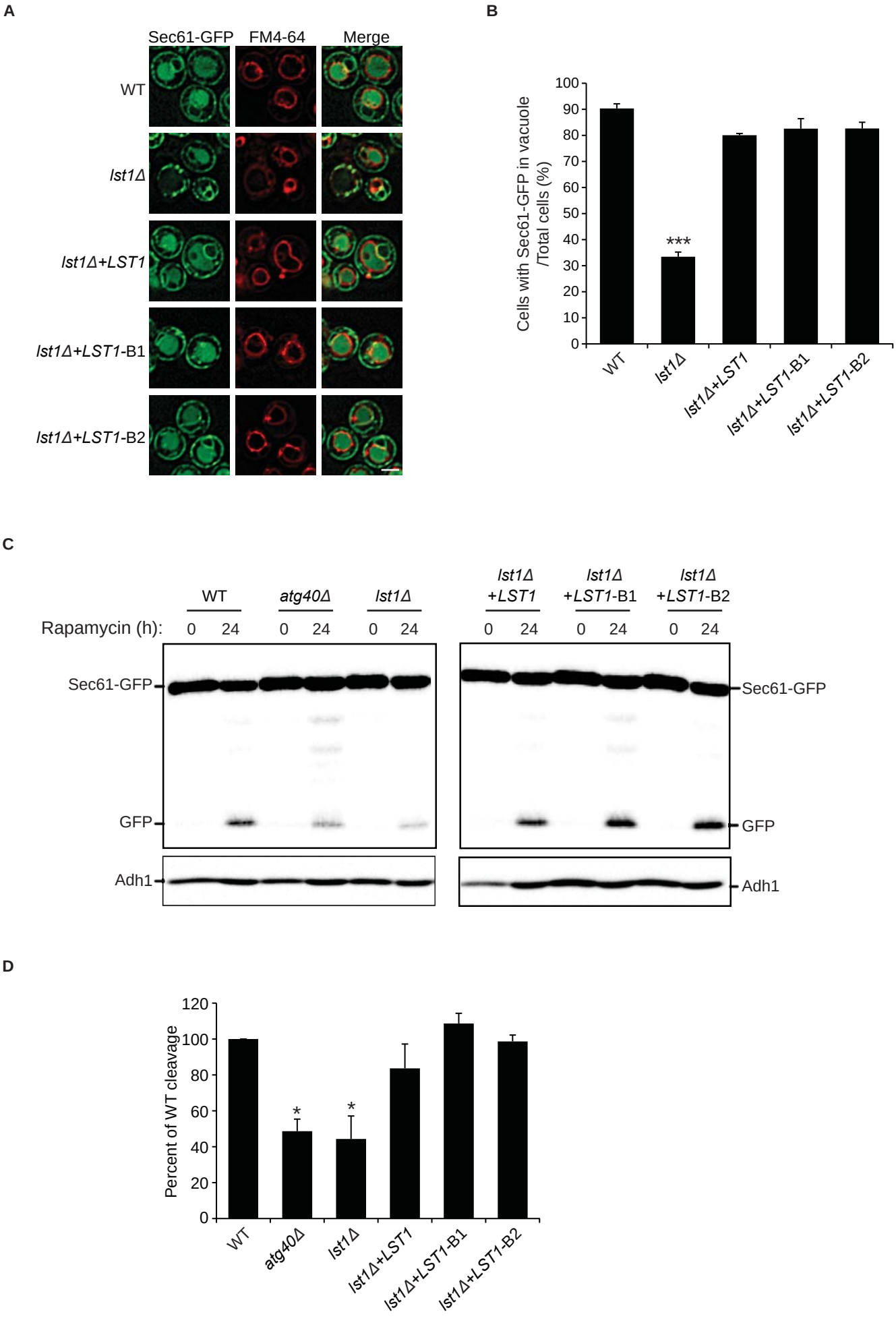
A
Sec61-GFP
FM4-64
Merge
WT
lst1Δ
lst1Δ+LST1
lst1Δ+LST1-B1
lst1Δ+LST1-B2
B
Cells with Sec61-GFP in vacuole /Total cells (%)
***
WT
lst1Δ
lst1Δ+LST1
lst1Δ+LST1-B1
lst1Δ+LST1-B2
C
WT
atg40Δ
lst1Δ
lst1Δ +LST1
lst1Δ +LST1-B1
lst1Δ +LST1-B2
Rapamycin (h):
0 24 0 24 0 24 0 24 0 24 0 24
Sec61-GFP
GFP
Adh1
D
Percent of WT cleavage
*
*
WT
atg40Δ
lst1Δ
lst1Δ+LST1
lst1Δ+LST1-B1
lst1Δ+LST1-B2

Figure S5. Lst1 plays distinct roles in ER-to-Golgi traffic and ER-phagy.
(**A**) The vacuolar degradation of Sec61-GFP was examined by fluorescence microscopy in WT, *lst1Δ* and *lst1Δ* mutant cells expressing WT *LST1* or *LST1* mutations, *LST1-B1*(K543M, R545M) or *LST1*-B2 (R219A, R224A). Scale bar, 5μm. (**B**) The percent of cells with Sec61-GFP delivered to the vacuole was quantitated from 300 cells. (**C**) The cleavage of Sec61-GFP to GFP was analyzed by immunoblotting using anti-GFP antibody. A representative blot from one of three experiments is shown. (**D**) Quantitation of the results in (**C**). WT was set to 100%. Error bars in (**B**) and (**D**) represent S.E.M., N=3; *P < 0.05, *** P < 0.001, Student's unpaired t-test.

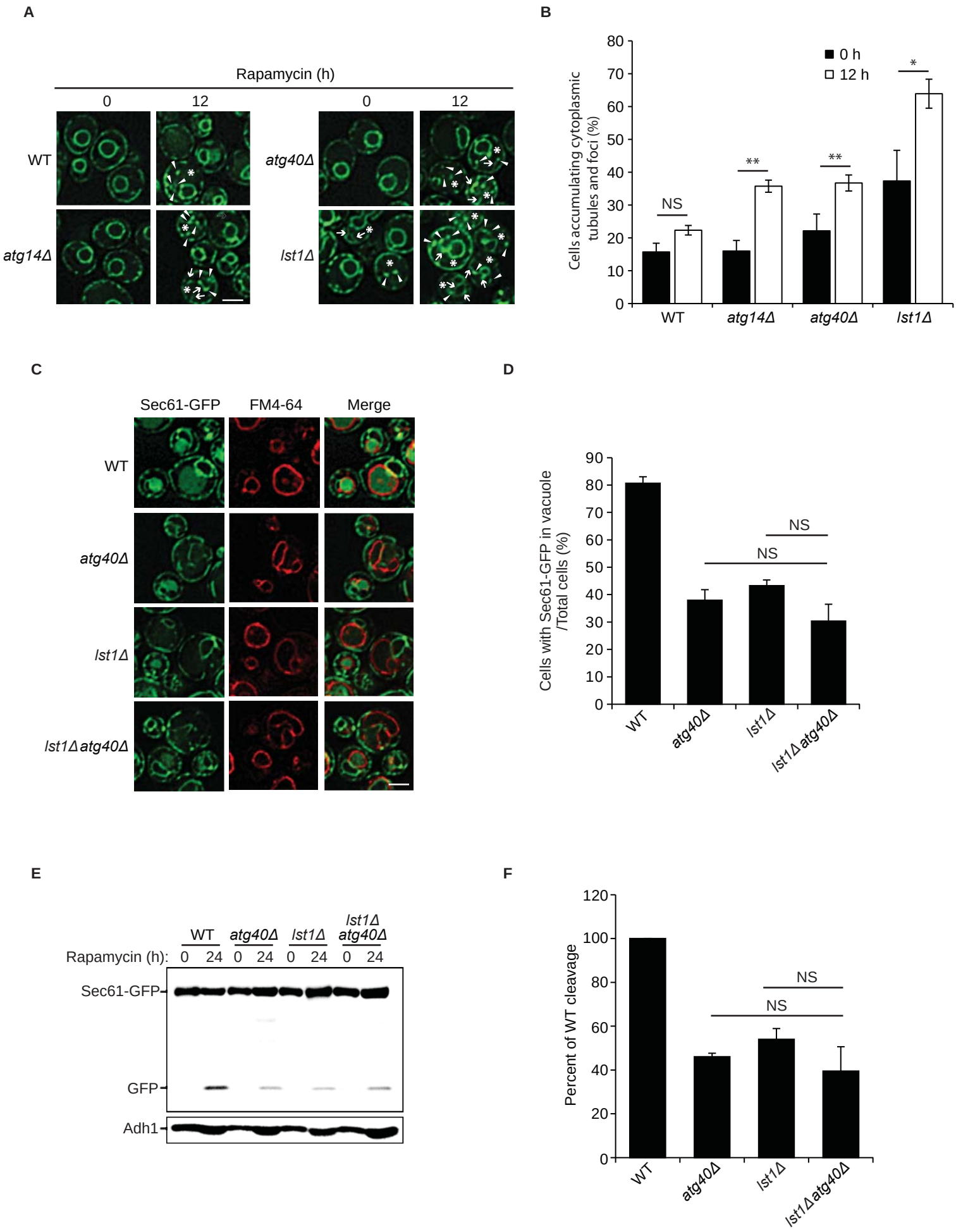
A
Rapamycin (h)
0
12
0
12
WT
atg40Δ
atg14Δ
lst1Δ
B
Cells accumulating cytoplasmic tubules and foci (%)
0 h
12 h
NS
**
**
*
WT
atg14Δ
atg40Δ
lst1Δ
C
Sec61-GFP
FM4-64
Merge
WT
atg40Δ
lst1Δ
lst1Δ atg40Δ
D
Cells with Sec61-GFP in vacuole /Total cells (%)
NS
NS
WT
atg40Δ
lst1Δ
lst1Δ atg40Δ
E
WT
atg40Δ
lst1Δ
lst1Δ atg40Δ
Rapamycin (h): 0 24 0 24 0 24 0 24
Sec61-GFP
GFP
Adh1
F
Percent of WT cleavage
NS
NS
WT
atg40Δ
lst1Δ
lst1Δ atg40Δ

Figure S6. Lst1 and Atg40 function together during ER-phagy.
(A) Representative images of WT, *atg14Δ, atg40Δ* and *lst1Δ* Sec61-GFP expressing cells before and after 12 h of rapamycin treatment. Cells were scored as positive (marked with asterisk) if they accumulated 2 or more cytoplasmic ER tubules and/or 2 or more foci of Sec61. Arrows mark accumulated tubules, while arrowheads mark accumulated foci. Sometimes foci were observed on tubules. (**B**) Quantitation of the images in **(A)** from three separate experiments. (**C**) The vacuolar delivery of Sec61-GFP was examined by fluorescence microscopy in WT, *atg40Δ*, *lst1Δ* and the *lst1Δatg40Δ* mutants. Scale bars in (**A)** and (**C**), 5 μm. (**D**) The percent of cells with Sec61-GFP delivered to the vacuole was quantitated in 300 cells. (**E**) The cleavage of Sec61-GFP to GFP was analyzed by immunoblotting using anti-GFP antibody. A representative blot from one of three experiments is shown. (**F**) Quantitation of the results in **(E)**. WT was set to 100%. Error bars in (**B**), (**D**) and (**F**) represent S.E.M., N=3. NS, not significant $P \geq 0.05$, *$P < 0.05$, * *$P < 0.01$, Student's unpaired t-test.

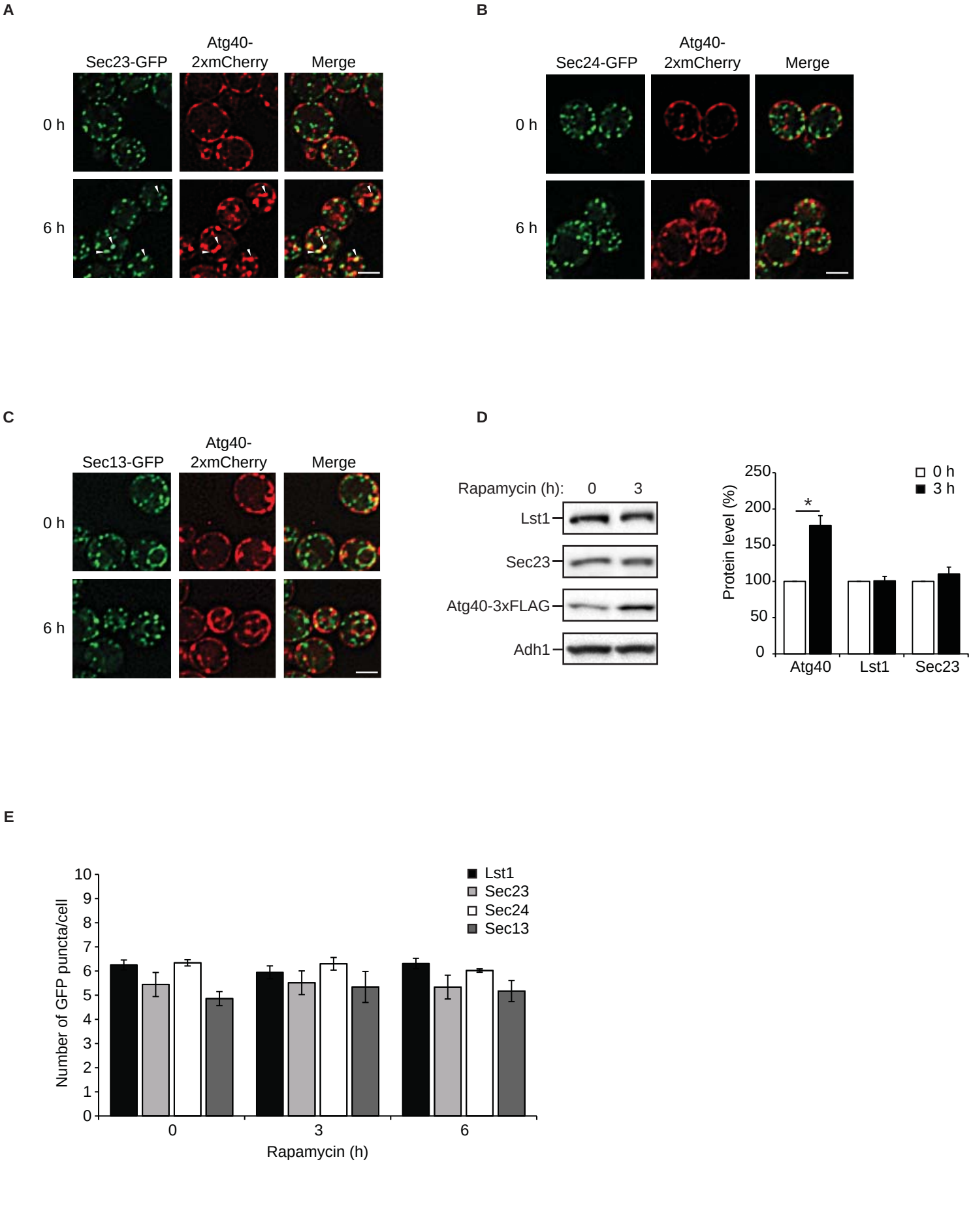
A
Sec23-GFP
Atg40-2xmCherry
Merge
0 h
6 h
B
Sec24-GFP
Atg40-2xmCherry
Merge
0 h
6 h
C
Sec13-GFP
Atg40-2xmCherry
Merge
0 h
6 h
D
Rapamycin (h): 0 3
Lst1
Sec23
Atg40-3xFLAG
Adh1
Protein level (%)
0 h
3 h
*
Atg40
Lst1
Sec23
E
Number of GFP puncta/cell
Lst1
Sec23
Sec24
Sec13
Rapamycin (h)

Figure S7. Sec23 colocalizes with Atg40 in rapamycin-treated cells
Representative images of cells expressing Sec23-GFP (**A**), Sec24-GFP (**B**), Sec13-GFP (**C**) and Atg40-2xmCherry at 0 and 6 h of rapamycin treatment. Arrowheads mark Sec23-GFP colocalizing with non-cortical Atg40-2xmCherry puncta. (**D**) Left, the expression of Lst1 and Sec23 does not increase during rapamycin treatment. Lysates were prepared by TCA lysis at 0 and 3 h after rapamycin treatment, and western blot analysis was performed. Right, quantitation of the data on the left, normalized to Adh1, from three separate experiments. (**E**) Bar graph showing the average number of Lst1-3xGFP, Sec23-GFP, Sec24-GFP and Sec13-GFP puncta at different times after rapamycin treatment. The quantitation was performed with at least 150 cells. Scale bars in (**A-C**), 5 μm. Error bars in (**D and E**) represent S.E.M., N=3. *P < 0.05, Student's unpaired t-test.

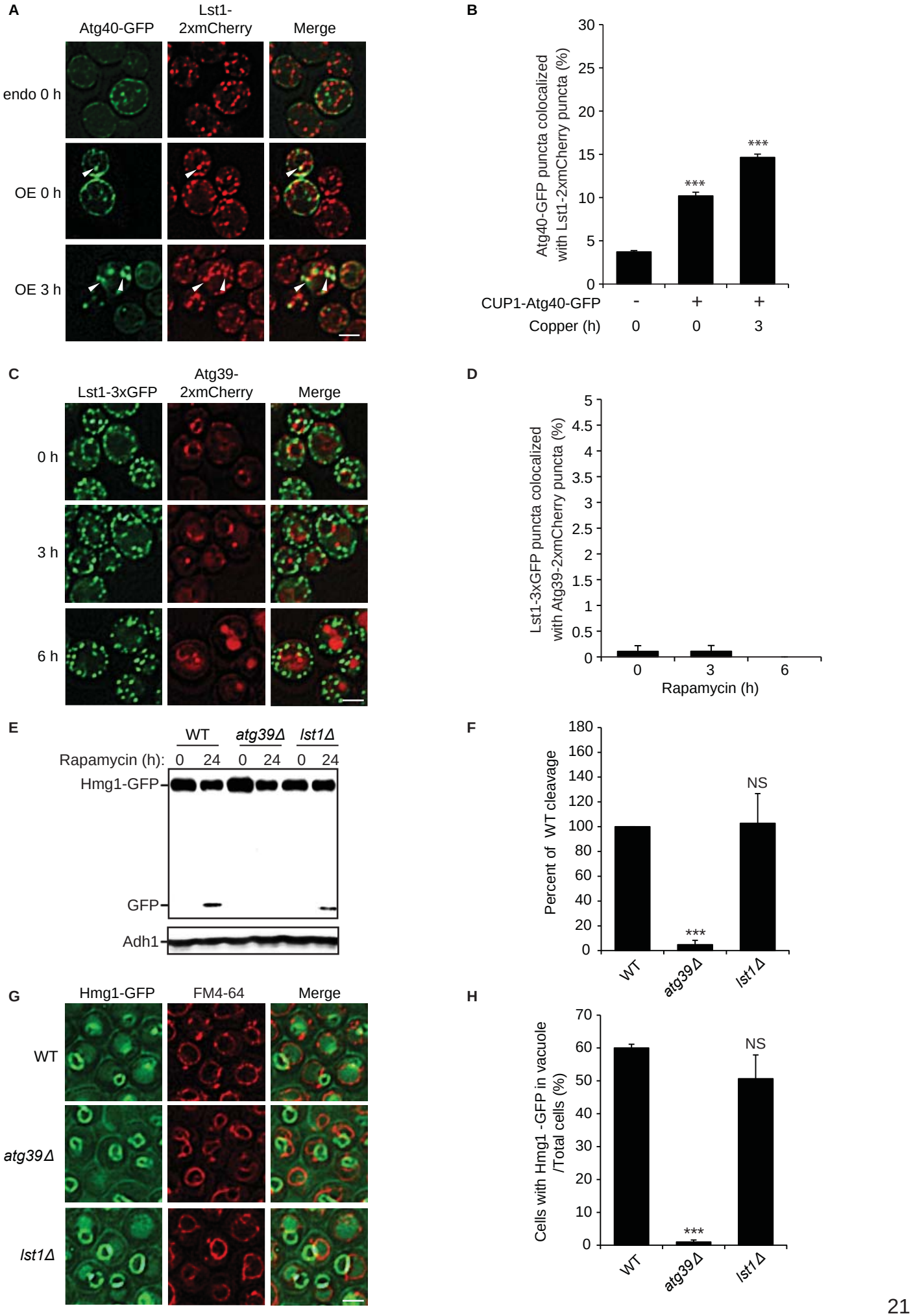
A
Atg40-GFP
Lst1-2xmCherry
Merge
endo 0 h
OE 0 h
OE 3 h
B
Atg40-GFP puncta colocalized with Lst1-2xmCherry puncta (%)
30
25
20
15
10
5
0
***
***
CUP1-Atg40-GFP - + +
Copper (h) 0 0 3
C
Lst1-3xGFP
Atg39-2xmCherry
Merge
0 h
3 h
6 h
D
Lst1-3xGFP puncta colocalized with Atg39-2xmCherry puncta (%)
5
4.5
4
3.5
3
2.5
2
1.5
1
0.5
0
0 3 6
Rapamycin (h)
E
WT atg39Δ lst1Δ
Rapamycin (h): 0 24 0 24 0 24
Hmg1-GFP
GFP
Adh1
F
Percent of WT cleavage
180
160
140
120
100
80
60
40
20
0
NS
***
WT
atg39Δ
lst1Δ
G
Hmg1-GFP
FM4-64
Merge
WT
atg39Δ
lst1Δ
H
Cells with Hmg1-GFP in vacuole /Total cells (%)
70
60
50
40
30
20
10
0
NS
***
WT
atg39Δ
lst1Δ

Figure S8. Lst1 does not appear to play a role in nuclear ER degradation.
(**A**) Representative images of cells expressing Atg40–GFP and Lst1-2xmCherry. Lst1-2xmCherry was expressed under its endogenous promoter, while Atg40–GFP was expressed either under its endogenous promoter (endo) or overexpressed (OE) using the *CUP1* promoter in the presence of 250 mM $CuSO_4$. Note that Atg40 overexpression was observed prior to the addition of copper to the medium (compare images in row 1 and row 2). (**B**) Quantitation of the results in **(A)** from three experiments. (**C**) Lst1 does not colocalize with Atg39. Representative images of cells expressing Lst1-3xGFP and Atg39-2xmCherry at different times after rapamycin treatment. (**D**) The percent of Lst1-3xGFP puncta colocalized with Atg39-2xmCherry puncta was quantitated from 150 cells. (**E**) The cleavage of Hmg1-GFP to GFP in WT and mutant strains was analyzed by immunoblotting using anti-GFP antibody. A representative blot is shown. (**F**) Three separate experiments were used to quantitate the ratio of free GFP to Hmg1-GFP from the data in **(E)**. WT was set to 100%. (**G**) The translocation of Hmg1-GFP to the vacuole was examined by fluorescence microscopy in WT and mutant cells 24 h after rapamycin treatment. FM4-64 was used to stain the vacuolar membrane. (**H**) The percent of cells with Hmg1-GFP delivered to the vacuole was quantitated by fluorescence from 300 cells. Scale bars in (**A**), (**C**) and (**G**), 5 μm. Error bars in (**B**), (**D**) (**F**) and (**H**) represent S.E.M., N=3. NS, not significant $P \geq 0.05$, *** $P < 0.001$, Student's unpaired t-test.

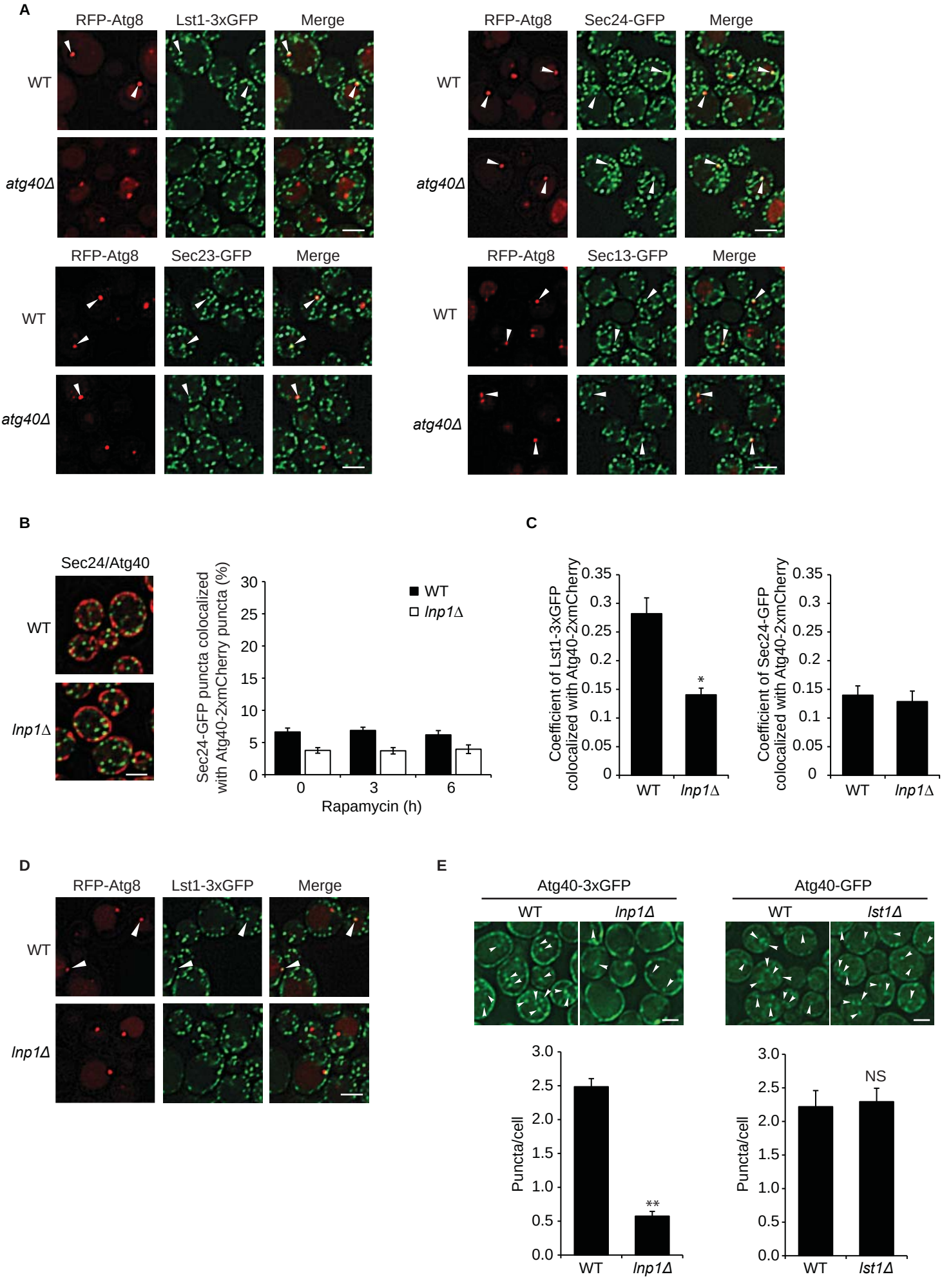
A
RFP-Atg8
Lst1-3xGFP
Merge
WT
atg40Δ
RFP-Atg8
Sec24-GFP
Merge
WT
atg40Δ
RFP-Atg8
Sec23-GFP
Merge
WT
atg40Δ
RFP-Atg8
Sec13-GFP
Merge
WT
atg40Δ
B
Sec24/Atg40
WT
lnp1Δ
Sec24-GFP puncta colocalized with Atg40-2xmCherry puncta (%)
30
25
20
15
10
5
0
WT
lnp1Δ
0
3
6
Rapamycin (h)
C
Coefficient of Lst1-3xGFP colocalized with Atg40-2xmCherry
0.35
0.3
0.25
0.2
0.15
0.1
0.05
0
*
WT
lnp1Δ
Coefficient of Sec24-GFP colocalized with Atg40-2xmCherry
0.35
0.3
0.25
0.2
0.15
0.1
0.05
0
WT
lnp1Δ
D
RFP-Atg8
Lst1-3xGFP
Merge
WT
lnp1Δ
E
Atg40-3xGFP
WT
lnp1Δ
Atg40-GFP
WT
lst1Δ
Puncta/cell
3.0
2.5
2.0
1.5
1.0
0.5
0.0
**
WT
lnp1Δ
Puncta/cell
3.0
2.5
2.0
1.5
1.0
0.5
0.0
NS
WT
lst1Δ

Figure S9. Lst1 does not colocalize with Atg40 or Atg8 in the *lnp1Δ* mutant.
(**A**) Representative images for Fig. 2D. Cells expressing RFP-Atg8 with Lst1-3xGFP, or Sec24-GFP, Sec23-GFP and Sec13-GFP were treated with rapamycin for 3 h. (**B**) Rapamycin does not induce the colocalization of Sec24 with Atg40. Sec24-GFP puncta colocalizing with Atg40-2xmCherry puncta in WT and the *lnp1Δ* mutant were quantitated. Left, representative images of cells treated with rapamycin for 6 h. Right, bar graph showing the percent of Sec24-GFP puncta colocalizing with Atg40-2xmCherry puncta at the indicated times after rapamycin treatment. (**C**) Bar graphs, quantitated by Volocity image analysis software, showing the Pearson's coefficient of Lst1-3xGFP (left) or Sec24-GFP (right) with Atg40-2xmCherry in WT and the *lnp1Δ* mutant 6h after rapamycin treatment. Fifty cells were analyzed in each experiment. (**D**) Representative images for Fig. 2F. Cells expressing RFP-Atg8 and Lst1-3xGFP were treated with rapamycin for 3 h. Scale bars in (**A**), (**B**) and (**D**), 5 μm. (**E**) Atg40 puncta distribution is unaltered in the *lst1Δ* mutant. Top, cells expressing Atg40-3xGFP or Atg40-GFP were treated for 3 h with rapamycin. Arrowheads mark Atg40 puncta. Bottom, quantitation of Atg40 puncta. Scale bars in (**E**), 2 μm. Error bars in (**B**), (**C**) and (**E**) represent S.E.M., N=3. NS, not significant $P \geq 0.05$, *$P < 0.05$, ** $P < 0.01$, Student's unpaired t-test.

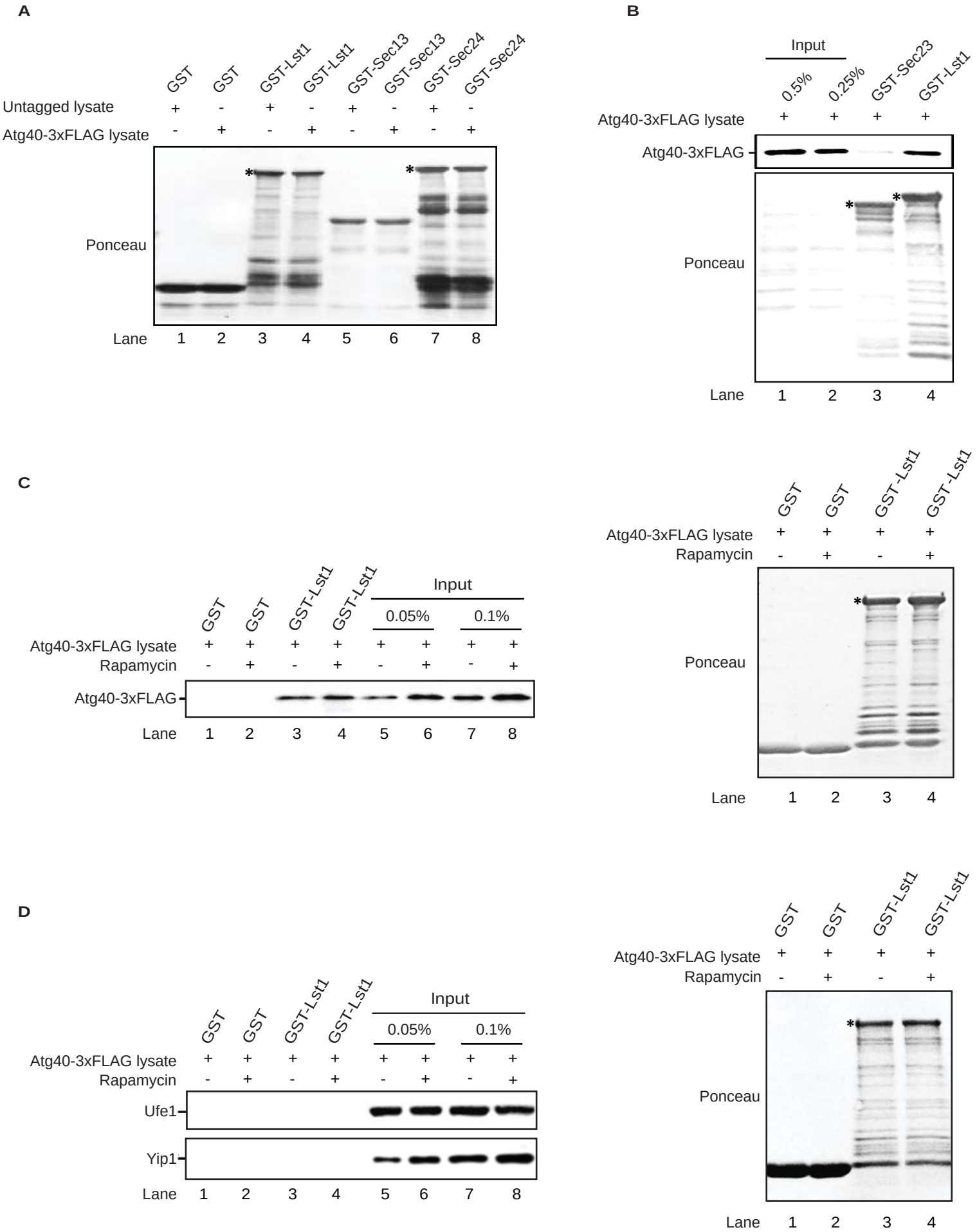
A
GST
GST
GST-Lst1
GST-Lst1
GST-Sec13
GST-Sec13
GST-Sec24
GST-Sec24
Untagged lysate
Atg40-3xFLAG lysate
Ponceau
Lane 1 2 3 4 5 6 7 8
B
Input
0.5%
0.25%
GST-Sec23
GST-Lst1
Atg40-3xFLAG lysate
Atg40-3xFLAG
Ponceau
Lane 1 2 3 4
C
GST
GST
GST-Lst1
GST-Lst1
Input
0.05%
0.1%
Atg40-3xFLAG lysate
Rapamycin
Atg40-3xFLAG
Lane 1 2 3 4 5 6 7 8
GST
GST
GST-Lst1
GST-Lst1
Atg40-3xFLAG lysate
Rapamycin
Ponceau
Lane 1 2 3 4
D
GST
GST
GST-Lst1
GST-Lst1
Input
0.05%
0.1%
Atg40-3xFLAG lysate
Rapamycin
Ufe1
Yip1
Lane 1 2 3 4 5 6 7 8
GST
GST
GST-Lst1
GST-Lst1
Atg40-3xFLAG lysate
Rapamycin
Ponceau
Lane 1 2 3 4

Figure S10. Lst1 selectively binds Atg40.
(**A**) Ponceau-S staining of blot shown in Fig. 3A. (**B**) Lst1, but not Sec23, binds Atg40. Equimolar amounts (0.1 μM) of purified recombinant GST-Lst1 and GST-Sec23 were incubated with 2mg of yeast lysate prepared from Atg40-3xFLAG tagged cells that had been treated with rapamycin. The beads were washed, and western blot analysis was performed using anti-FLAG antibody. (**C**) Left, same as **(B)** except lysates were prepared from Atg40-3xFLAG tagged cells that were untreated or treated with rapamycin. Right, Ponceau-S staining of the blot shown on the left. (**D**) Left, western blot analysis was performed on the samples in **(C)** using anti-Ufe1 and anti-Yip1 antibodies. Right, Ponceau-S staining of the blot shown on the left. Asterisks in (**A**-**D**) mark full length GST-Lst1, GST-Sec24 and GST-Sec23 fusion protein bands.

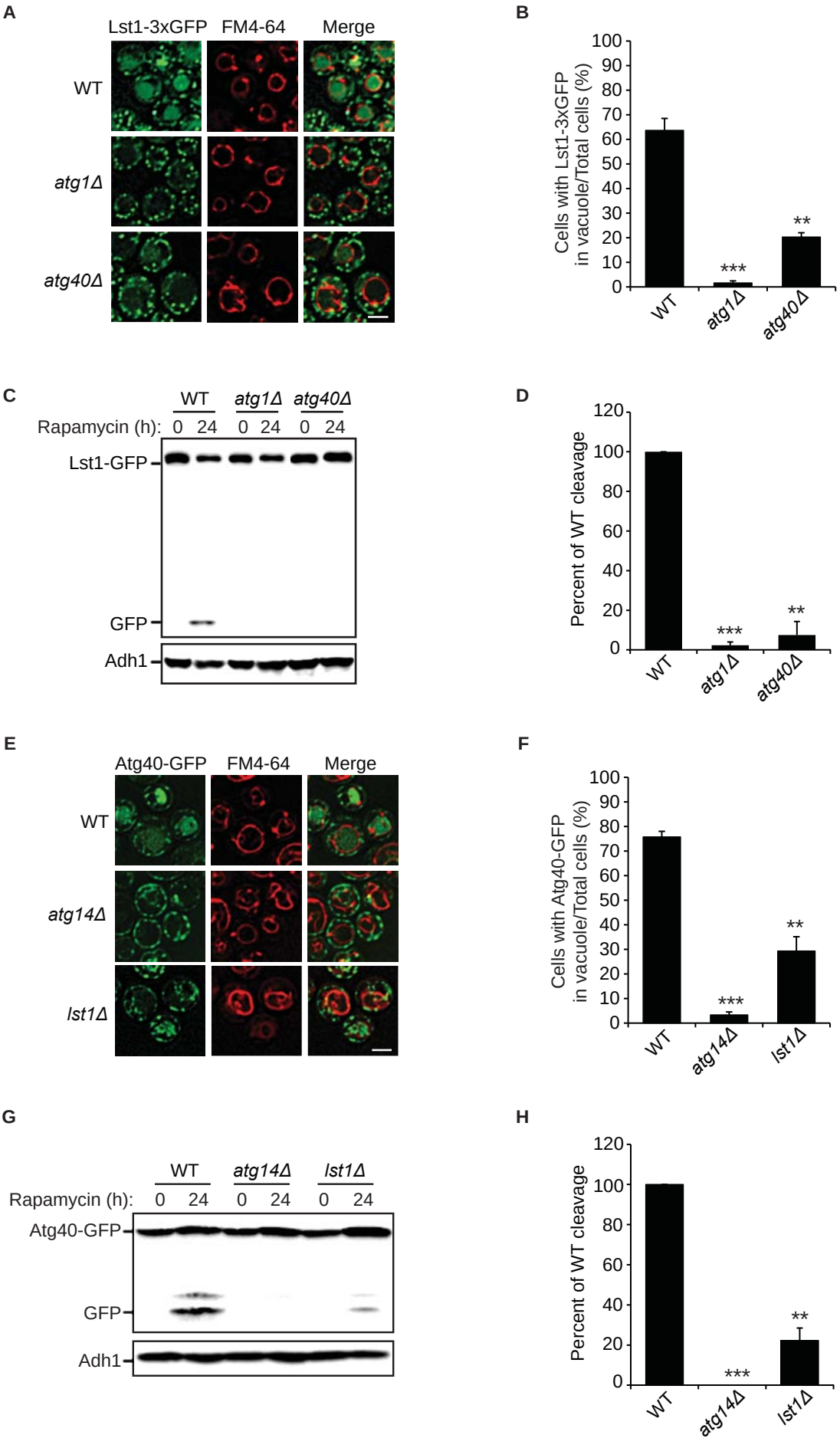
A
Lst1-3xGFP
FM4-64
Merge
WT
atg1Δ
atg40Δ
B
Cells with Lst1-3xGFP in vacuole/Total cells (%)
100
90
80
70
60
50
40
30
20
10
0
**
***
WT
atg1Δ
atg40Δ
C
WT
atg1Δ
atg40Δ
Rapamycin (h):
0
24
0
24
0
24
Lst1-GFP
GFP
Adh1
D
Percent of WT cleavage
120
100
80
60
40
20
0
**
***
WT
atg1Δ
atg40Δ
E
Atg40-GFP
FM4-64
Merge
WT
atg14Δ
lst1Δ
F
Cells with Atg40-GFP in vacuole/Total cells (%)
100
90
80
70
60
50
40
30
20
10
0
**
***
WT
atg14Δ
lst1Δ
G
WT
atg14Δ
lst1Δ
Rapamycin (h):
0
24
0
24
0
24
Atg40-GFP
GFP
Adh1
H
Percent of WT cleavage
120
100
80
60
40
20
0
**
***
WT
atg14Δ
lst1Δ

Figure S11. Lst1 degradation is dependent on Atg40, and Atg40 degradation depends on Lst1 in rapamycin-treated cells.
(**A)** The translocation of Lst1-3xGFP to the vacuole was examined by fluorescence microscopy in WT, *atg1Δ* and *atg40Δ* cells 24 h after rapamycin treatment. (**B**) The percent of cells with Lst1-3xGFP delivered to the vacuole was quantitated by fluorescence from 300 cells. (**C**) The degradation of Lst1-GFP to GFP was analyzed by immunoblotting using anti-GFP antibody, and a representative blot from three separate experiments is shown. Adh1 was used as a loading control. (**D**) Quantitation of the cleavage of Lst1-GFP to GFP in WT and mutant cells from three separate experiments. WT was set to 100%. (**E**) The delivery of Atg40-GFP to the vacuole was examined by fluorescence microscopy in WT, *atg14Δ* and *lst1Δ* cells 24 h after rapamycin treatment. (**F**) The data in **(E)** were quantitated from 300 cells in three separate experiments. (**G**) The cleavage of Atg40-GFP to GFP was analyzed in WT, *atg14Δ* and *lst1Δ* mutants by immunoblotting with anti-GFP antibody and a representative blot is shown. (**H**) The results in **(G)** were quantitated from three separate experiments. Scale bars in (**A**) and (**E**), 5 μm. Error bars in (**B**), (**D**), (**F**) and (**H**) represent S.E.M., N=3-6; ** $P < 0.01$; ***$P < 0.001$, Student's unpaired t-test.

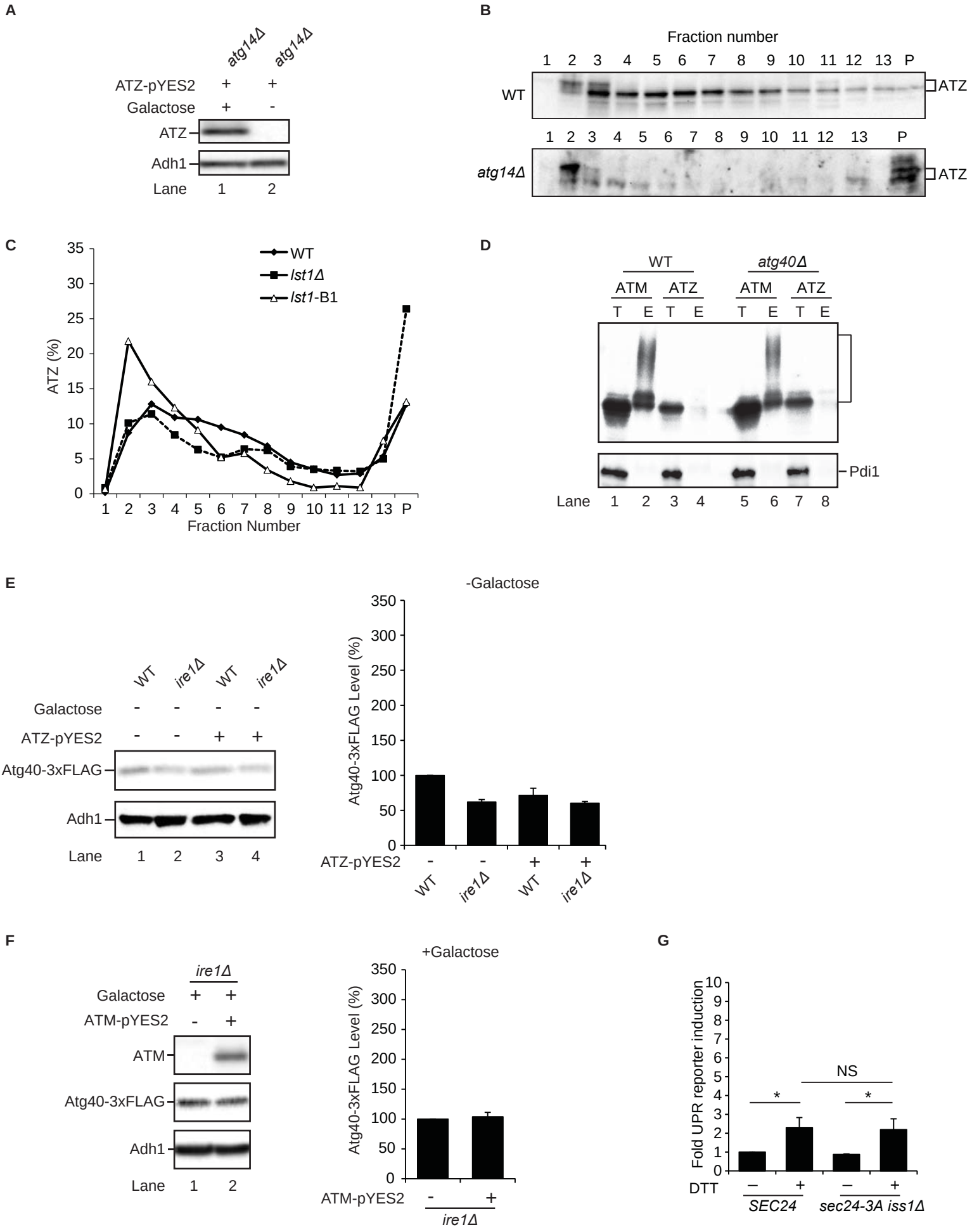
A
atg14Δ
atg14Δ
ATZ-pYES2 + +
Galactose + -
ATZ
Adh1
Lane 1 2
B
Fraction number
1 2 3 4 5 6 7 8 9 10 11 12 13 P
WT
ATZ
1 2 3 4 5 6 7 8 9 10 11 12 13 P
atg14Δ
ATZ
C
WT
lst1Δ
lst1-B1
ATZ (%)
Fraction Number
D
WT
atg40Δ
ATM ATZ ATM ATZ
T E T E T E T E
Pdi1
Lane 1 2 3 4 5 6 7 8
E
-Galactose
WT ire1Δ WT ire1Δ
Galactose - - - -
ATZ-pYES2 - - + +
Atg40-3xFLAG
Adh1
Lane 1 2 3 4
Atg40-3xFLAG Level (%)
ATZ-pYES2 - - + +
WT ire1Δ WT ire1Δ
F
+Galactose
ire1Δ
Galactose + +
ATM-pYES2 - +
ATM
Atg40-3xFLAG
Adh1
Lane 1 2
Atg40-3xFLAG Level (%)
ATM-pYES2 - +
ire1Δ
G
Fold UPR reporter induction
NS
* *
DTT – + – +
SEC24
sec24-3A iss1Δ

Figure S12. ATM, but not ATZ, is secreted.
(**A**) ATZ is only expressed in the presence of galactose. ATZ expression was monitored in *atg14Δ* mutant cells from plasmid ATZ-pYES2 in the presence of 2% galactose (lane 1) or 2% glucose (lane 2). (**B**) Blots used to graph Fig. 4A. Microsomal membrane fractions were prepared by lysing WT (top) and the *atg14Δ* mutant (bottom), in the presence of detergent, and then fractionated on a sucrose gradient. Gradient fractions were blotted with antibody directed against ATZ. Soluble ATZ was at the top of the gradient and aggregates reside in the pellet (P). (**C**) ATZ was analyzed in sucrose gradients in WT, *lst1Δ,* and *lst1*-B1 cells. The *lst1*-B1 mutant was examined on 3 separate gradients. The data shown are from one experiment that was representative of the average. (**D)** Top, Total (T) and external (E) fractions were assayed for ATM or ATZ. Similar results were obtained with WT, *atg40Δ* and *lst1Δ* cells. The data for WT and *atg40Δ* are shown. The bracket marks high molecular weight alpha-1 antitrypsin (ATM) that is glycosylated in the Golgi and secreted into the extracellular space (*50*). ATZ, which is targeted to the vacuole, is not secreted. Approximately 5% of the total ATM was secreted. High molecular weight ATM is only visualized in the external, and not in the total, fraction because it is 18x more concentrated than the total. Bottom, the ER luminal resident protein, protein disulfide isomerase (Pdi1), was assayed in all fractions by western blot analysis. (**E**) Atg40 upregulation is dependent on ATZ expression. Atg40 levels were measured by western blot analysis as in Fig. 5A-B, only the cells were grown in glucose, which did not induce ATZ expression. The loss of Ire1 only increased Atg40 expression in galactose grown cells (Fig. 5A-B). Glucose deprivation, which likely slows glycosylation and protein folding in the ER, is a known source of ER stress (*52*). The data on the right were normalized to Adh1 from three separate experiments. (**F**) ATM overexpression does not upregulate the expression of Atg40. Atg40 levels were measured by western blot analysis in *ire1Δ* mutant cells that contain overexpressed ATM (lane 2) or an empty vector (lane 1). The data on the right were normalized to Adh1 from three separate experiments. (**G**) The induction of the UPR was assayed by flow cytometry in cells harboring the 4xUPRE-GFP gene in the absence or presence of 8 mM DTT. Greater than 30,000 cells were analyzed for each strain. S.E.M., N=3; NS, not significant $P \geq 0.05$, *$P < 0.05$, Student's unpaired t-test.

A

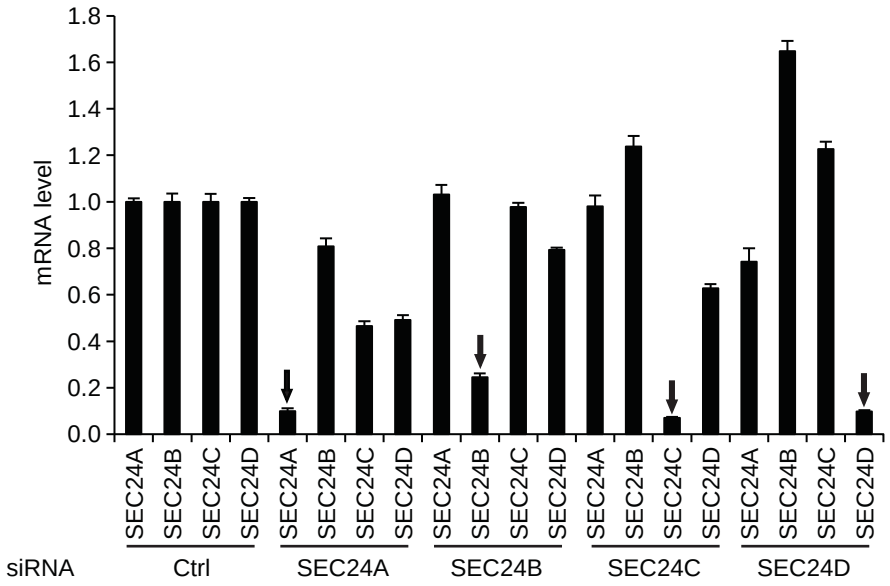
mRNA level
1.8
1.6
1.4
1.2
1.0
0.8
0.6
0.4
0.2
0.0
SEC24A
SEC24B
SEC24C
SEC24D
siRNA
Ctrl
SEC24A
SEC24B
SEC24C
SEC24D

B

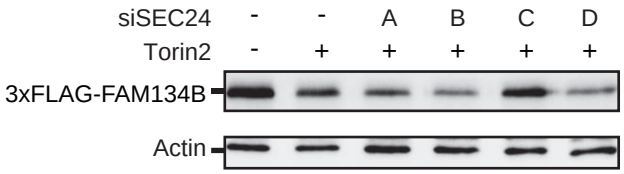
siSEC24 - - A B C D
Torin2 - + + + + +
3xFLAG-FAM134B
Actin

C

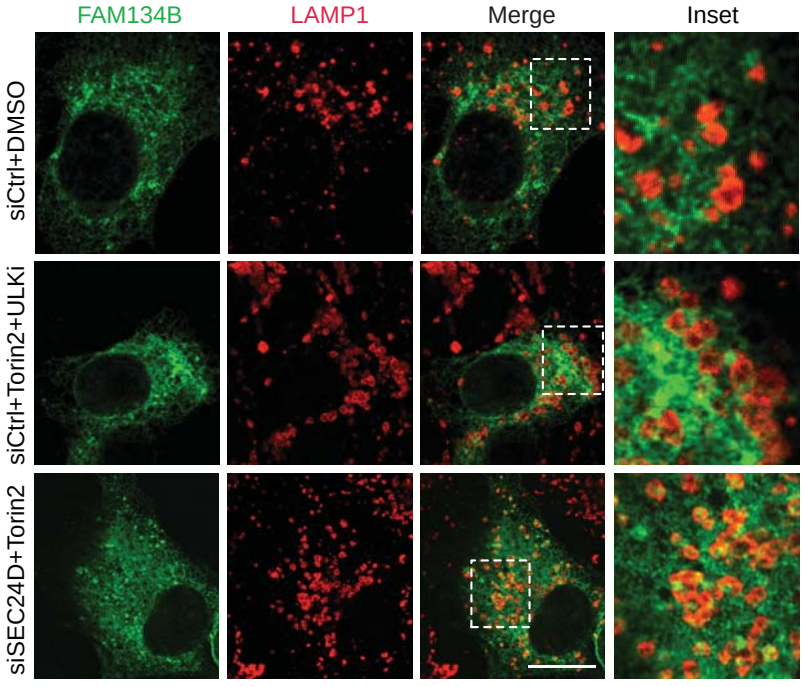
FAM134B
LAMP1
Merge
Inset
siCtrl+DMSO
siCtrl+Torin2+ULKi
siSEC24D+Torin2

Figure S13. SEC24C is required for the degradation of FAM134B during ER-phagy.
(**A**) qRT-PCR was used to assess the depletion of the different SEC24 isoforms. The data shown are normalized to actin mRNA levels. (**B**) 3xFLAG-FAM134B degradation was monitored, by western blot analysis, in lysates prepared from Torin2 treated control siRNA or SEC24 siRNA depleted U2OS cells. Actin was used as a loading control. (**C**) Representative images of siRNA control (Ctrl) cells treated with DMSO (top row) and siSEC24D depleted cells treated with Bafilomycin A1 and Torin2 (bottom row). The siRNA Ctrl cells in the middle row were treated with Bafilomycin A1, Torin 2 and MRT68921, a ULK1/2 inhibitor (ULKi). Scale bar is 10μm.

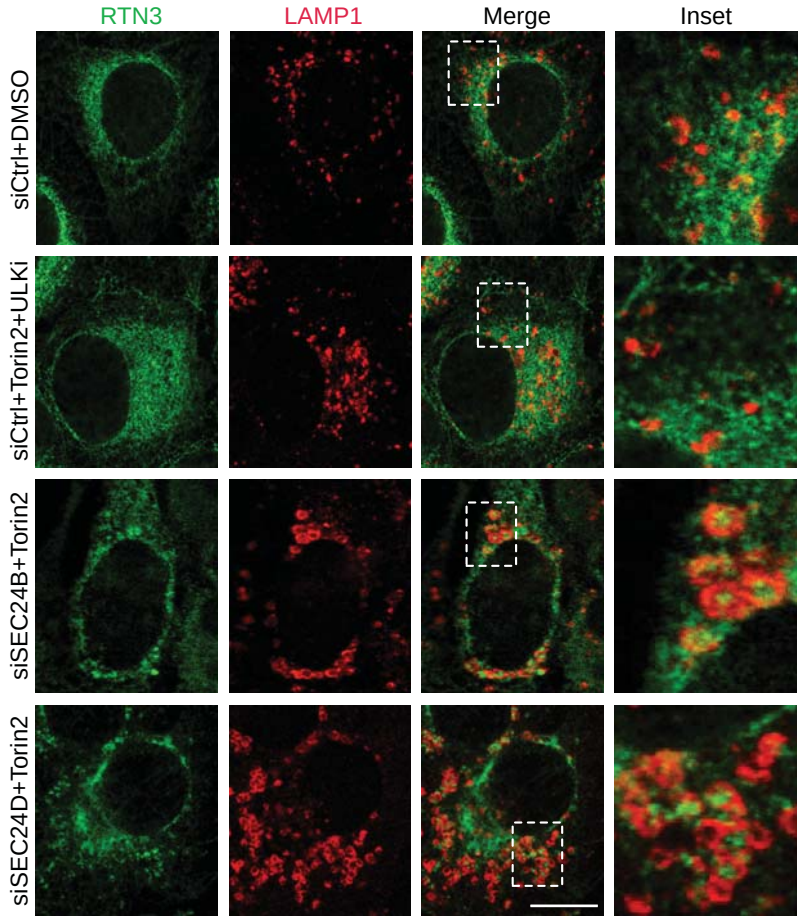

Figure S14. SEC24B and SEC24D are not required for the delivery of RTN3 to the lysosome. Representative images of siRNA depleted cells. Top row, siRNA control (Ctrl) treated with DMSO. All other samples were treated with Bafilomycin A1 and Torin2. The Ctrl cells in the second row were also treated with MRT68921 (ULKi). Scale bar is 10μm.

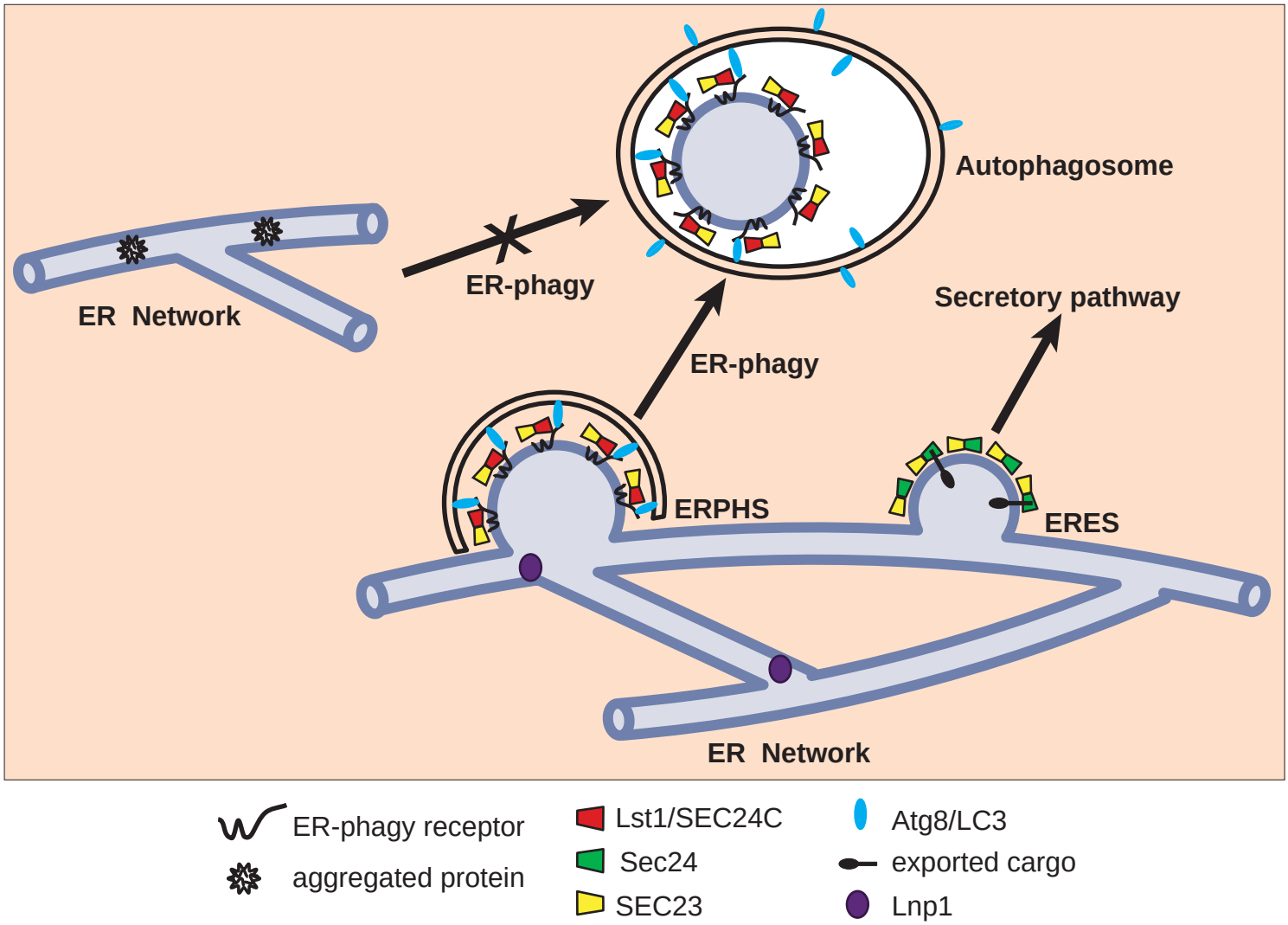

Figure S15. COPII coat subunits mediate two different pathways from the ER, the secretory and ER-phagy pathways.
Proteins that traffic through the secretory pathway exit the ER via **ER exit sites** (**ERES**) in canonical COPII vesicles that contain Sec24-Sec23. In response to drugs that inhibit TOR or ER stress caused by aggregation-prone secretory proteins, ER domains are targeted for degradation via **ER-phagy sites** (**ERPHS**) that contain Lst1-Sec23 in yeast and SEC24C-SEC23 in mammals. **ERPHS** do not form in the absence of Lnp1, an ER protein that resides at the three-way junctions and stabilizes them. In yeast, ER-phagy induction leads to the association of the Lst1-Sec23 complex with puncta that contain the ER-phagy receptor, Atg40, and its binding partner Atg8, a ubiquitin-like protein required for autophagosome formation. In mammals, SEC24C-SEC23 may perform an analogous role. The RTN3 interactome analysis (33) supports an interaction between RTN3 and the SEC24C-SEC23 complex. Both isoforms of SEC23 (SEC23A and SEC23B) are part of the RTN3 interactome (33). Besides RTN3, SEC24C-SEC23 may interact with other ER-phagy receptors.

Supplementary Table S1. Key yeast strains used in this study.

Strain Number	Genotype	Source
SFNY 2714	*MATα ura3-52 leu2-3, 112 his3Δ200 SEC61-GFP::URA3*	Ferro-Novick Lab Collection
SFNY 2837	*MATa ura3-52 leu2-3, 112 his3Δ200 atg40Δ::KanMX6 SEC61-GFP::LEU2*	Ferro-Novick Lab Collection
SFNY 2824	*MATα sec24Δ::LEU2 iss1Δ::KanMX6 ade2-1 can-100 his3-11, 15 trp1-1 leu2-3, 112 ura3-1 pSFNB2054 (Sec24 T324A/T325A/T328A, CEN, HIS3) SEC61-GFP::URA3*	This study
SFNY 3404	*MATα ura3-52 leu2-3, 112 his3Δ200 iss1Δ::KanMX6 SEC61-GFP::URA3*	This study
SFNY 3193	*MATa ura3-52 leu2-3, 112 his3Δ200 lst1Δ::His3MX6 pho8::pho8Δ60 (URA3) SEC61-GFP::LEU2*	This study
SFNY 3113	*MATa ura3-52 leu2-3, 112 his3Δ200 PER33-GFP::LEU2*	This study
SFNY 3115	*MATa ura3-52 leu2-3, 112 his3Δ200 atg40Δ::KanMX6 PER33-GFP::LEU2*	This study
SFNY 3276	*MATa ura3-52 leu2-3, 112 his3Δ200 lst1Δ::His3MX6 pho8::pho8Δ60 (URA3) PER33-GFP::LEU2*	This study
SFNY 3363	*MATa ura3-52 leu2-3, 112 his3Δ200 ATG40-2xmCherry::URA3 LST1-3xGFP::LEU2*	This study
SFNY 2955	*MATa ura3-52 leu2-3, 112 his3Δ200 ATG40-3xFLAG::KanMX6*	This study
SFNY 3172	*MATα ura3-52 leu2-3, 112 his3Δ200 LST1-3xGFP::URA3*	This study
SFNY 3173	*MATα ura3-52 leu2-3, 112 his3Δ200 atg1Δ::His3MX6 LST1-3xGFP::URA3*	This study
SFNY 3213	*MATα ura3-52 leu2-3, 112 his3Δ200 LST1-3xGFP::URA3 atg40Δ::KanMX6*	This study
SFNY 3429	*MATa ura3-52 leu2-3, 112 his3Δ200 LST1-GFP::KanMX6*	This study
SFNY 3430	*MATα ura3-52 leu2-3, 112 his3Δ200 atg1Δ::His3MX6 LST1-GFP::KanMX6*	This study
SFNY 3431	*MATa ura3-52 leu2-3, 112 his3Δ200 atg40Δ::KanMX6 LST1-GFP::His3MX6*	This study
SFNY 3326	*MATα ura3-52 leu2-3, 112 his3Δ200 pep4Δ::KanMX6 SEC61-GFP::LEU2*	This study
SFNY 3387	*MATα ura3-52 leu2-3, 112 his3Δ200 atg14Δ::His3MX6 SEC61-GFP::URA3 pep4Δ::KanMX6*	This study
SFNY 3327	*MATa ura3-52 leu2-3, 112 his3Δ200 atg40Δ::KanMX6 pep4Δ::His3MX6 SEC61-GFP::LEU2*	This study
SFNY 3353	*MATa ura3-52 leu2-3, 112 his3Δ200 lst1Δ::His3MX6 pho8::pho8Δ60 (URA3) SEC61-GFP::LEU2 pep4Δ::KanMX6*	This study
SFNY 3406	*MATα ura3-52 leu2-3, 112 his3Δ200 4xUPRE-GFP::URA3*	This study
SFNY 3423	*MATα ura3-52 leu2-3, 112 his3Δ200 hrd1Δ::His3MX6 4xUPRE-GFP::URA3*	This study
SFNY 3411	*MATα ura3-52 leu2-3, 112 his3Δ200 atg39Δ::His3MX6 4xUPRE-GFP::URA3*	This study
SFNY 3410	*MATa ura3-52 leu2-3, 112 his3Δ200 atg40Δ::KanMX6 4xUPRE-GFP::URA3*	This study
SFNY 3407	*MATα ura3-52 leu2-3, 112 his3Δ200 lst1Δ::His3MX6 4xUPRE-GFP::URA3*	This study

SFNY 2823	*MATα sec24Δ::LEU2 iss1Δ::KanMX6 ade2-1 can-100 his3-11, 15 trp1-1 leu2-3, 112 ura3-1 pSFNB1915 (SEC24, CEN, HIS3) SEC61-GFP::URA3*	This study
SFNY 2717	*MATα his3Δ1 leu2Δ0 ura3Δ0 met15Δ0 hrr25Δ::KanMX6 pSFNB1715 (HRR25, CEN, LEU2) SEC61-GFP::URA3*	This study
SFNY 2716	*MATα his3Δ1 leu2Δ0 ura3Δ0 met15Δ0 hrr25Δ::KanMX6 pSFNB1871 (hrr25-5, CEN, LEU2) SEC61-GFP::URA3*	This study
SFNY 2659	*MATα his3-200 leu2-3, 112 ura3-52 pSFNB1637 (GFP-ATG8, CEN, URA3)*	This study
SFNY 2835	*MATα ura3-52 leu2-3, 112 his3Δ200 atg1Δ::His3MX6 pSFNB1637 (GFP-ATG8, CEN, URA3)*	This study
SFNY 3405	*MATα ura3-52 leu2-3, 112 his3Δ200 lst1Δ::His3MX6 pSFNB1637 (GFP-ATG8, CEN, URA3)*	This study
SFNY 2076	*MATa ura3-52 leu2-3, 112 his3Δ200 pho8::pho8Δ60 (URA3)*	This study
SFNY 2979	*MATα ura3-52 leu2-3, 112 his3Δ200 atg1Δ::His3MX6 pho8::pho8Δ60 (URA3)*	This study
SFNY 2942	*MATa ura3-52 leu2-3, 112 his3Δ200 lst1Δ::His3MX6 pho8::pho8Δ60 (URA3)*	This study
SFNY 3152	*MATα ura3-52 leu2-3, 112 his3Δ200 PEX14-GFP::KanMX6*	This study
SFNY 3157	*MATα ura3-52 leu2-3, 112 his3Δ200 atg36Δ::His3MX6 PEX14-GFP::KanMX6*	This study
SFNY 3153	*MATα ura3-52 leu2-3, 112 his3Δ200 lst1Δ::His3MX6 PEX14-GFP::KanMX6*	This study
SFNY 3142	*MATα ura3-52 leu2-3, 112 his3Δ200 OM45-GFP::KanMX6*	This study
SFNY 3147	*MATα ura3-52 leu2-3, 112 his3Δ200 atg32Δ::His3MX6 OM45-GFP::KanMX6*	This study
SFNY 3143	*MATα ura3-52 leu2-3, 112 his3Δ200 lst1Δ::KanMX6 OM45-GFP::His3MX6*	This study
SFNY 3355	*MATα ura3-52 leu2-3, 112 his3Δ200 lst1Δ::KanMX6 SEC61-GFP::URA3 pRS313-LST1 (CEN, HIS3)*	This study
SFNY 3356	*MATα ura3-52 leu2-3, 112 his3Δ200 lst1Δ::KanMX6 SEC61-GFP::URA3 pRS313-LST1-B1 (K543M/R545M, CEN, HIS3)*	This study
SFNY 3357	*MATα ura3-52 leu2-3, 112 his3Δ200 lst1Δ::KanMX6 SEC61-GFP::URA3 pRS313-LST1-B2 (R219A/R224A, CEN, HIS3)*	This study
SFNY 3367	*MATa ura3-52 leu2-3, 112 his3Δ200 ATG40-2xmCherry::URA3 SEC24-GFP::LEU2*	This study
SFNY 3425	*MATα ura3-52 leu2-3, 112 his3Δ200 ATG39-2xmCherry::URA3 LST1-3xGFP::LEU2*	This study
SFNY 3194	*MATa ura3-52 leu2-3, 112 his3Δ200 lst1Δ::His3MX6 pho8::pho8Δ60 (URA3) SEC61-GFP::LEU2 atg40Δ::KanMX6*	This study
SFNY 3412	*MATα sec24Δ::LEU2 iss1Δ::KanMX6 ade2-1 can-100 his3-11, 15 trp1-1 leu2-3, 112 ura3-1 pSFNB1915 (SEC24, CEN, HIS3) 4xUPRE-GFP::URA3*	This study
SFNY 3413	*MATα sec24Δ::LEU2 iss1Δ::kanMX6 ade2-1 can-100 his3-11, 15 trp1-1 leu2-3, 112 ura3-1 pSFNB2054 (Sec24 T324A/T325A/T328A, CEN, HIS3) 4xUPRE-GFP::URA3*	This study
SFNY 1841	*MATa ura3-52 leu2-3, 112 his3Δ200*	Ferro-Novick Lab Collection
SFNY 1842	*MATα ura3-52 leu2-3, 112 his3Δ200*	Ferro-Novick Lab Collection

SFNY 2836	*MATa ura3-52 leu2-3, 112 his3Δ200 atg40Δ::KanMX6*	Ferro-Novick Lab Collection
SFNY 3140	*MATα ura3-52 leu2-3, 112 his3Δ200 lst1Δ::His3MX6*	This study
SFNY 3446	*MATa ura3-52 leu2-3, 112 his3Δ200 ATG40-3xFLAG::KanMX6 pNB660 (CEN, URA3)*	This study
SFNY 3447	*MATa ura3-52 leu2-3, 112 his3Δ200 ATG40-3xFLAG::KanMX6 ATZ-pYES2 (2u, URA3)*	This study
SFNY 3448	*MATa ura3-52 leu2-3, 112 his3Δ200 ATG40-3xFLAG::KanMX6 atg14Δ:: His3MX6 pNB660 (CEN, URA3)*	This study
SFNY 3449	*MATa ura3-52 leu2-3, 112 his3Δ200 ATG40-3xFLAG::KanMX6 atg14Δ:: His3MX6 ATZ-pYES2 (2u, URA3)*	This study
SFNY 3451	*MATa ura3-52 leu2-3, 112 his3Δ200 ATG40-3xFLAG::KanMX6 ire1Δ:: His3MX6 pNB660 (CEN, URA3)*	This study
SFNY 3452	*MATa ura3-52 leu2-3, 112 his3Δ200 ATG40-3xFLAG::KanMX6 ire1Δ:: His3MX6 ATZ-pYES2 (2u, URA3)*	This study
SFNY 3458	*MATα ura3-52 leu2-3, 112 his3Δ200 ATG40-GFP::KanMX6*	This study
SFNY 3459	*MATα ura3-52 leu2-3, 112 his3Δ200 lst1Δ::His3MX6 ATG40-GFP::KanMX6*	This study
SFNY 3460	*MATα ura3-52 leu2-3, 112 his3Δ200 ATG40-GFP::KanMX6 atg14Δ:: His3MX6*	This study
SFNY 3461	*MATα ura3-52 leu2-3, 112 his3Δ200 LST1-3xGFP::URA3 RFP-ATG8-pRS315 (CEN, LEU2)*	This study
SFNY 3462	*MATα ura3-52 leu2-3, 112 his3Δ200 SEC24-GFP::URA3 RFP-ATG8-pRS315 (CEN, LEU2)*	This study
SFNY 3463	*MATa ura3-52 leu2-3, 112 his3Δ200 LST1-3xGFP::URA3 atg40Δ::KanMX6 RFP-ATG8-pRS315 (CEN, LEU2)*	This study
SFNY 3464	*MATa ura3-52 leu2-3, 112 his3Δ200 SEC24-GFP::URA3 atg40Δ::KanMX6 RFP-ATG8-pRS315 (CEN, LEU2)*	This study
SFNY 2088	*MATa ura3-52 leu2-3, 112 his3Δ200 RTN1-GFP::KanMX6*	Ferro-Novick Lab Collection
SFNY 3139	*MATa ura3-52 leu2-3, 112 his3Δ200 atg40Δ::KanMX6 RTN1-GFP::LEU2*	Ferro-Novick Lab Collection
SFNY 3427	*MATα ura3-52 leu2-3, 112 his3Δ200 lst1Δ::KanMX6 RTN1-GFP:: His3MX6*	This study
SFNY 3160	*MATα sec24Δ::LEU2 iss1Δ::KanMX6 ade2-1 can-100 his3-11, 15 trp1-1 leu2-3, 112 ura3-1 pSFNB1915 (SEC24, CEN, HIS3) PEX14-GFP::TRP1*	This study
SFNY 3161	*MATα sec24Δ::LEU2 iss1Δ::kanMX6 ade2-1 can-100 his3-11, 15 trp1-1 leu2-3, 112 ura3-1 pSFNB2054 (Sec24 T324A/T325A/T328A, CEN, HIS3) PEX14-GFP::TRP1*	This study
SFNY 3150	*MATα sec24Δ::LEU2 iss1Δ::KanMX6 ade2-1 can-100 his3-11, 15 trp1-1 leu2-3, 112 ura3-1 pSFNB1915 (SEC24, CEN, HIS3) OM45-GFP::TRP1*	This study
SFNY 3151	*MATα sec24Δ::LEU2 iss1Δ::kanMX6 ade2-1 can-100 his3-11, 15 trp1-1 leu2-3, 112 ura3-1 pSFNB2054 (Sec24 T324A/T325A/T328A, CEN, HIS3) OM45-GFP::TRP1*	This study
SFNY 2903	*MATα ura3-52 leu2-3,112 his3Δ200 atg14::His3MX6 SEC61-GFP::URA3*	This study
SFNY 3390	*MATa ura3-52 leu2-3,112 his3Δ200 lnp1::KanMX6 ATG40-2xmCherry::URA3 Lst1-3xGFP::LEU2*	This study
SFNY 3391	*MATa ura3-52 leu2-3,112 his3Δ200 lnp1::KanMX6 ATG40-2xmCherry::URA3 Sec24-GFP::LEU2*	This study

SFNY 3483	*MATα ura3-52 leu2-3, 112 his3Δ200 LST1-2mCherry::LEU2 pCUP1-Atg40-GFP-pRS426 (2u, URA3)*	This study
SFNY 3484	*MATα ura3-52 leu2-3, 112 his3Δ200 ATG40-GFP::His3MX6 LST1-2mCherry::LEU2*	This study
SFNY 3485	*MATa ura3-52 leu2-3, 112 his3Δ200 SEC13-GFP::URA3 ATG40-2mCherry::LUE2*	This study
SFNY 3486	*MATa ura3-52 leu2-3, 112 his3Δ200 SEC23-GFP::URA3 ATG40-2mCherry::LUE2*	This study
SFNY 3487	*MATα ura3-52 leu2-3, 112 his3Δ200 SEC23-GFP::URA3 RFP-ATG8-pRS315 (CEN, LEU2)*	This study
SFNY 3488	*MATa ura3-52 leu2-3, 112 his3Δ200 atg40::KanMX6 SEC23-GFP::URA3 RFP-ATG8-pRS315 (CEN, LEU2)*	This study
SFNY 3489	*MATα ura3-52 leu2-3, 112 his3Δ200 SEC13-GFP::URA3 RFP-ATG8-pRS315 (CEN, LEU2)*	This study
SFNY 3490	*MATa ura3-52 leu2-3, 112 his3Δ200 atg40::KanMX6 SEC13-GFP::URA3 RFP-ATG8-pRS315 (CEN, LEU2)*	This study
SFNY 3491	*MATa ura3-52 leu2-3, 112 his3Δ200 ATG40-3xFLAG::KanMX6 pho23::His3MX6*	This study
SFNY 3492	*MATa ura3-52 leu2-3, 112 his3Δ200 ATG40-3xFLAG::KanMX6 rpd3::His3MX6*	This study
SFNY 3494	*MATa ura3-52 leu2-3, 112 his3Δ200 lnp1::KanMX6 LST1-3XGFP::URA3 RFP-ATG8-pRS315 (CEN, LEU2)*	This study
SFNY 3221	*MATa ura3-52 leu2-3, 112 his3Δ200 HMG1-GFP::KanMX6*	This study
SFNY 3222	*MATα ura3-52 leu2-3, 112 his3Δ200 atg39Δ::His3MX6 HMG1-GFP::LEU2*	This study
SFNY 3388	*MATα ura3-52 leu2-3, 112 his3Δ200 lst1Δ::KanMX6 HMG1-GFP::LEU2*	This study

Supplementary Table S2. List of siRNAs used in this study.

Name	Target Gene	Company	Catalog No.	Target sequence
siCtrl	Control	Dharmacon (siGenome Non-Targeting siRNA Pool)	D-001206-13-05	
siSEC24A	SEC24A	Dharmacon (siGenome-SMARTpool)	M-024405-01-0005	CCAAGAAGGUAUUACAUCA CAAAUGCACGUCUAGAUGA GGAAACUUCUUUGUUAGGU GGUUGUAUUUCUCGGUAUU
siSEC24B	SEC24B	Dharmacon (siGenome-SMARTpool)	M-008299-01-0006	GGGAAAGGCUGUGACAAUA GACCAGAAGUUCAGAAUUC CAGGGUGCAUCUAUUAUUA CCAGAUUCAUUUCGGUGUA
siSEC24C#1	SEC24C	Dharmacon (siGenome-SMARTpool)	M-008467-01-0007	GCAAACGUGUGGAUGCUUA CAGGGAAGCUCUUUCUAUU UGGCUGAUCUAUAUCGAAA CUGUAUAUGAUUCGGUAUU
siSEC24C#2	SEC24C	Qiagen (Flexitube siRNA)	SI00713965	CCCGUUGAGAGUACUACCGAA
siSEC24D	SEC24D	Dharmacon (siGenome-SMARTpool)	M-008493-01-0008	GAGGAACCCUUUACAAAUA GACCAGAGAUCUCAACUGA GUACAUGAAUUGCUUGUUG GGUAAAUCACGGCGAGAGU